RADC-TR-77-348
Final Report
October 1977

TECHNOLOGY AND PHYSICS OF INFRARED AND POINT CONTACT DIODES

Department of Physics
Massachusetts Institute of Technology
Cambridge, Massachusetts 02139

Sponsored by
Defense Advanced Research Projects Agency
ARPA Order No. 2618

ROME AIR DEVELOPMENT CENTER
AIR FORCE SYSTEMS COMMAND
GRIFFIS AIR FORCE BASE, NEW YORK 13441

TECHNOLOGY AND PHYSICS OF INFRARED
AND POINT CONTACT DIODES

Contractor: Massachusetts Institute of Technology
Contract Number: F19628-74-C-0182
Effective Date of Contract 24 January 1974
Contract Expiration Date: 31 May 1977

ARPA Order No.: 2618
Program Code Number: 5D10
Period of Work Covered: 1 May 1974 - 31 May 1977
Principal Investigator: Ali Javan
Phone: 617-253-5088
Project Engineer: Dr. Richard Picard
Phone: 617-861-4927

This technical report has been reviewed and is approved.

R. H. Picard

RICHARD H. PICARD
Contract Monitor

Unclassified
SECURITY CLASSIFICATION OF THIS PAGE (When Data Entered)

19 REPORT DOCUMENTATION PAGE

READ INSTRUCTIONS BEFORE COMPLETING FORM

1. REPORT NUMBER: 18 RADC-TR-77-348

2. GOVT ACCESSION NO.: 9

3. RECIPIENT'S CATALOG NUMBER: rept.

4. TITLE (and Subtitle): 6 TECHNOLOGY AND PHYSICS OF INFRARED AND POINT CONTACT DIODES.

5. TYPE OF REPORT & PERIOD COVERED: Final 5/1/74-5/31/77

6. PERFORMING ORG. REPORT NUMBER: 1 May 74-31 May 77

7. AUTHOR(s): 10 Ali Javan

8. CONTRACT OR GRANT NUMBER(s): 15 F19628-74-C-0182, ARPA Order-2618

9. PERFORMING ORGANIZATION NAME AND ADDRESS:
Department of Physics
Massachusetts Institute of Technology
Cambridge, MA 02139

10. PROGRAM ELEMENT, PROJECT, TASK AREA & WORK UNIT NUMBERS: 16 2001 17 01-01
61101E

11. CONTROLLING OFFICE NAME AND ADDRESS:
Defense Advanced Research Project Agency
1400 Wilson Boulevard
Arglinton, VA 22209

12. REPORT DATE: 11 Oct[redacted]r [redacted]77

13. NUMBER OF PAGES: 95

14. MONITORING AGENCY NAME & ADDRESS (if different from Controlling Office):
Deputy for Electronic Technology (RADC)
Hanscom AFB, Massachusetts 01773
Monitor/Richard Picard/ESO

15. SECURITY CLASS. (of this report): Unclassified

15a. DECLASSIFICATION/DOWNGRADING SCHEDULE:

16. DISTRIBUTION STATEMENT (of this Report)

Approved for public release; distribution unlimited.

12 95p.

17. DISTRIBUTION STATEMENT (of the abstract entered in Block 20, if different from Report)

18. SUPPLEMENTARY NOTES

This research was sponsored by the Defense Advanced Research Projects Agency, ARPA Order 2618

19. KEY WORDS (Continue on reverse side if necessary and identify by block number)

Tunneling resonances, dielectric formation, oxide studies, photoemission.

20. ABSTRACT (Continue on reverse side if necessary and identify by block number)

Preliminary work in this laboratory has shown that tunneling characteristics of metal-oxide-metal junctions are essentially independent of frequency as long as photon energy is less than the barrier height. Recent calculations show the effects of circuit parameters on response of antenna/diode combinations; the junction capacitance is responsible for roll off in the infrared. Capacitance reduction requires shrinking junction

DD FORM 1 JAN 73 1473 EDITION OF 1 NOV 65 IS OBSOLETE
S/N 0102-LF-014-6601

Unclassified
SECURITY CLASSIFICATION OF THIS PAGE (When Data Entered)

401 735

Cont. Block No. 20

size, hence the need for micron and submicron geometries. Photo emission (over the barrier rather than tunneling) and thermal effects dominate the response in the visible region. It seems likely that photoemission is a fast effect and can be used for visible mixing. Calculation of operating parameters for an infrared antenna/diode combination has been completed. This shows the performance of the receiving and detecting elements as a function of geometry and dielectric constants; included is the effect of the strong frequency dependence of the circuit elements. This work will be prepared for publication. Additional measurements have been made of the antenna pattern of a printed antenna/diode. An unsuccessful search was conducted for negative resistance in a fine tungsten point on gold. Low temperature measurements were made on several vacuum deposited diodes. Junction characteristics in radiation whose photon energy is greater than the barrier height were measured and results were analyzed. A journal article based on this work has been published.

Important elements of device merit are junction non-linearity and negative resistance. These are being demonstrated in small, high-speed junctions capable of operation in the infrared. The effects may be further enhanced by choice of meterials, techniques of application, and operating temperature.

ACCESSION for		
NTIS	White Section	X
DDC	Buff Section	☐
UNANNOUNCED		☐
JUSTIFICATION		
BY		
DISTRIBUTION/AVAILABILITY CODES		
Dist.	AVAIL. and/or SPECIAL	
A		

TABLE OF CONTENTS

INTRODUCTION

Preliminary work in this laboratory has shown that tunneling characteristics of metal-oxide-metal junctions are essentially independent of frequency as long as photon energy is less than the barrier height. Recent calculations show the effects of circuit parameters on response of antenna/diode combinations; the junction capacitance is responsible for roll off in the infrared. Capacitance reduction requires shrinking junction size, hence the need for micron and submicron geometries. Photo emission (over the barrier rather than tunneling) and thermal effects dominate the response in the visible region. It seems likely that photoemission is a fast effect and can be used for visible mixing. Calculation of operating parameters for an infrared antenna/diode combination has been completed. This shows the performance of the receiving and detecting elements as a function of geometry and dielectric constants; included is the effect of the strong frequency dependence of the circuit elements. This work will be prepared for publication. Additional measurements have been made of the antenna pattern of a printed antenna/diode. An unsuccessful search was conducted for negative resistance in a fine tungsten point on gold. Low temperature measurements were made on several vacuum deposited diodes. Junction characteristics in radiation whose photon energy is greater than the barrier height were measured and results were analyzed. A journal article based on this work has been published.

Important elements of device merit are junction non-linearity and negative resistance. These are being demonstrated in small, high-speed junctions capable of operation in the infrared. The effects

may be further enhanced by choice of materials, techniques of application, and operating temperature.

SECTION 1: Techniques for Evaporating Junctions using a Metal Mask

a. Diodes fabricated by evaporation through a mask

Early in the contract in order to facilitate testing of different materials and fabrication procedures, we made a number of relatively large area junctions by evaporation through a mask. An etched metal mask was procured. (See Fig. 1). The design is such that when an evaporation is made the substrate may be oxidized, then rotated 90° in its holder, without breaking vacuum, and a second evaporation crosses each narrow oxidized metal strip with another equally thin metal strip, thus simultaneously forming four tunneling barriers.

Work with aluminum-aluminum oxide-lead barriers of about $100(\mu m)^2$ area showed that with short oxidation times at relatively low pressures it is possible to achieve oxide thickness under 10 Å but that exposure of the finished product to air increased the barrier resistance an order of magnitude in the first few minutes and ultimately to values above a megohm. Since this change did not take place in the vacuum, and the metal layer (about 5000 Å) overlying the junction is rather too thick for penetration, it would seem that the process proceeds from the edges. Even larger area junctions also having a few hundred ohms junction resistance, hence thicker oxide, were relatively stable in the room environment. Additional work has been done with aluminum as the top metal as well as the bottom. The same increases in resistance were noted. When silicon monoxide was evaporated over the junction before breaking vacuum, the increase could be reduced to a few percent per day. It is likely that even greater stabilization may be achieved either by varying the thickness of silicon monoxide or depositing it

from two points to assure covering the exposed edges of the junction, which might otherwise be shadowed, or by using a different protective material.

The junctions appear quite non-linear at 0.1 to 0.2 V bias. A corresponding non-linearity is observed when the junctions are driven at 10 MHz. Our calculations indicate that these relatively large area junctions should exhibit about the same non-linearity at X-band and that roll-off should not exclude detecting a signal at 337 μm. The microwave signal was barely discernable and we did not see the infrared signal although 10 mw of incident power was available. The most likely reason is poor coupling into the junction. It is well to recall that these junctions are on the order of 100 square μm as opposed to 0.1 square μm, as is the limit of conventional photolithography.

b. Dielectric Formation

Much consideration has been given to methods of dielectric formation since the problems are unique when thicknesses of the order 10 Å are required. As these are less than 10 atom layers thick and permit essentially no pinholes, self-grown oxides (or possibly nitrides or sulfides) appear to be the most promising approach. Insulators that are evaporated, sputtered or deposited in some other way tend to form small islands which grow both in size and thickness to cover the surface. Such layers inherently have pinholes until their thickness is several hundred Å.

c. Oxide Studies

In an effort to understand oxide growth mechanisms and means of evaluating thickness and perfection of such dielectric layers,

we contacted Perkin Elmer Optical Products Group. They proposed a program to study oxidation rates using ESCA (Electron Spectroscopy for Chemical Analysis) which should also give help in detecting pinholes too small (< 30 Å) to see with a field emission source scanning electron microscope. They also proposed to look for the effect of atmospheric exposure to the surfaces and evaluate metal cleaning techniques preparatory to oxidation. They are prepared to evaluate evaporated, and subsequently processed, metal to determine the thickness, uniformity and composition of the barrier in our diodes.

d. Metal Oxidation Techniques

To study oxidation characteristics of nickel, several 20 μm x 20 μm junctions were fabricated. Nickel was evaporated first and the slide heated on the hot plate. Four runs gave the following resistances as a function of oxidation time.

Junction	Oxidation Time	Resistance Range
Ni-NiO-Pb	0 hours	short circuit
Ni-NiO-Pb	3 hours	81Ω - 130Ω
Ni-NiO-Ni	4 hours	680Ω - 910Ω
Ni-NiO-Pb	15 3/4 hours	320 KΩ - 900 KΩ

Resistances typically increased 25 percent in the 24 hours following their preparation.

A lead on tin junction was made with three hours of hot plate oxidation. Resistances were 4.3 KΩ and 8.2 KΩ . These increased by half in the 17 hours after fabrication. This junction should be operable in the high microwave region and as a negative resistance device below 3.5°K.

e. Solder Techniques

It has been known for many years that indium metal will wet glass and quartz.[1,2] This characteristic has been used very effectively in sample preparation for low temperature measurements.

We have found that the best contacts are made by the following procedure: Heat a small crucible of indium just above its melting point on a hot plate over night. This produces a small amount of oxide which is dissolved in the metal. Experiment has shown that stronger bonds are made with this oxide present. A clean pencil soldering iron on a variac set at 60-70 v is used to apply the indium. The tip must be free of lead and tin to obtain a good bond.

SECTION 2: Far Infrared

a. Non-coherent far infrared sources

Non-coherent far infrared sources tend to be very inefficient. The simplest of such sources being a heated black body with a short wavelength cutoff filter. Almost all of its energy will be of a wavelength shorter than desired and will be absorbed (or reflected) by the filter. Interestingly, a much more efficient source is a high pressure mercury lamp without pyrex outer jacket.[3] This emits high intensity ultra-violet and behaves as a 5000° far infrared radiator but at intermediate wavelengths (below about 100 μm) it has greatly decreased intensity. Two such lamps were purchased: General Electric H 100 A4/T and Philips HPK 125 W. A layer of black PVC tape was used as a filter against shorter wavelengths and significant radiation was observed both on calorimetric detectors and evaporated junctions.

b. Antenna designs

Several antenna arrays were built by Lincoln Labs for this project. The three designs studied under this contract consist of: 1) An infrared dipole and tunneling junction are connected to a microwave dipole. DC output is taken through a parallel conductor transmission line. (Fig. 2); 2) A $\frac{3\lambda}{2}$ infrared dipole with overlap junction and transmission line (Fig. 3). 3) Three small variations from $\frac{3\lambda}{2}$ infrared dipoles with crosses for junctions alternated with a $\lambda/2$, a pair of $\lambda/2$ separated by $\lambda/2$ (Fig. 4) and a $\frac{3\lambda}{2}$ antenna with overlap junction.

Shipley (positive) photoresist is used throughout this fabrication, in part because it gives overhanging edges after development, which facilitates the metal separation in a lift off process.

Substrates are sapphire on which resist is exposed and developed, leaving half dipole and half of a transmission line as uncovered sapphire. After chrome and nickel evaporation, the resist is stripped removing most of the metal and leaving the half pattern. The subsequent air oxidation may later be modified by a plasma operation. A second resist is exposed with the other half pattern and, for reduced resistance, some of the first half pattern is also overcoated. The plasma cleaning step removes residual resist and may modify the existing junction oxide. Chrome and gold are evaporated and the resist is again stripped leaving the desired final pattern.

c. Antenna Trimming

In another phase of the experiment the output of a far infrared HCN laser was coupled to a printed element with an integrated dipole antenna. The laser could be made to operate in either 337 μm or 311 μm transitions. The resulting rectified signals from both wavelengths were compared and it was found that sometimes one wavelength was coupled better than the other as a result of a different antenna mismatching. Changing the antenna length would modify the antenna impedance affecting the amount of infrared power actually reaching the non-linear junction. It was found that when trimming the antenna length with a diamond scribe in small steps, the rectified signal increased initially, reached a maximum and finally decreased for shorter dipole lengths. For 337 μm and 311 μm these maxima were correspondingly different.

d. Rotation of printed antenna elements in an infrared field

A mount for printed diodes has been made which provides contacts to the outputs and permits rotation of the antenna in the laser beam. This rotation may be either about the dipole element itself or about the feed lines (on the surface but perpendicular to the dipole elements); at all times the dipole remains properly oriented in the polarized laser field. Rotation about the feed lines of the $\frac{3\lambda}{2}$ element gives a large maximum and two very much smaller side lobes. (See Fig. 5). Rotation about the antenna elements gives a broad flat maximum with no side lobes. This has been interpreted as increased reflectivity of the underlying sapphire as the angle of incidence approached 90°. Calculations have been made which fit the data qualitatively (including the effects of the dielectric constant).

e. Antenna pattern study

The antenna pattern of a $\frac{\lambda}{2}$ printed nickel on chromium dioxide was measured at 337 μm. The maximum signal was displaced 30° from the normal to this apparently symmetric structure. Initial speculation was that reflections from the steel back-up plate were responsible, but a half inch hole cut in the plate did not significantly change the asymmetry. Sharper beam focusing and probing the surrounding substrate revealed that pickup and rectification by the measuring probes themselves accounted for some of the asymmetry and for troubles in attempting to focus on the junction. Work on an antenna pattern with gold overlay demonstrated that tungsten probes penetrating the metal film an appreciable distance formed ohmic contacts. It has been found that even slightly elevated

temperatures alter these junctions. As a result it was not possible to use conductive epoxy which requires heating for proper curing. The substrates were sapphire which is not wet by indium and so leads could not be fastened to the contact pads. To establish greater system symmetry a teflon lens was used instead of an off axis parabola.

SECTION 3: Cryogenics

a. Tunneling resonances

In addition to the normal electron tunneling that is the basis for the calculations described in Section 4 of this report other processes may take place. A tunneling electron may be inelastically scattered by an impurity in the dielectric;[4] the electron loses a certain amount of energy and the impurity molecule is left in an excited state with energy $h\nu$. This process can only occur if the junction is biased with a voltage $V_2 > h\nu/e$. As a result of this, a structure appears in the plot of $\frac{\partial^2 J}{\partial V^2}$ versus the bias voltage, which except for the background, is similar to the infrared spectrum of the impurity molecules in the gas phase. (See Fig. 6). Because of the thermal smearing of the Fermi level of the electrodes, the use of cryogenic temperatures is necessary in order to improve the resolution of the resulting tunneling spectrum. In this way, we have observed tunneling resonances in $Al-Al_2O_3-Pb$.

This effect can be utilized in different ways. As a spectroscopic tool for chemical analysis it can give information on the impurity content of the dielectric in the tunneling junction. On the other hand, the enhanced non-linearities that result when the junctions are cooled to cryogenic temperatures will improve the performance of the MOM junctions as mixer elements. Specifically, we are examining the possibilities of utilizing the non-linearities existing at low bias (a few mV) in non-superconducting tunneling due to "zero bias anomalies." In conjunction with the small RC of our junction it would considerably improve their rectifying and mixing characteristics in the infrared.

b. Repair of cryogenic equipment

The liquid helium dewar (with quartz windows) was returned to the manufacturer several times during the course of this contract for repairs. He found and repaired more than one leak each time. We seem to have developed a corrosion problem and have tried to prolong the life of the dewar by keeping it dry when not at low temperature. A second dewar with clear windows over 50% transparent to 10 μm radiation, but with a smaller working space, was used more often toward the end of the contract.

The flexible helium transfer tube also developed a leak and was repaired.

c. Superfluid helium

In an attempt to maintain junctions under test at a constant temperature the helium in the dewar was pumped. After increase in the size of the pumping line and of the pump, it became possible to pump the liquid helium to below the lambda point in about 40 minutes. Although there is a thermal match barrier between the junction and the helium subsequent work has demonstrated that superfluid helium (below the lambda point at 2.1°K) does maintain the sample at a much more uniform temperature than "normal" liquid helium.

d. Extension of laser lab

A tube and sets of mirrors have been installed from the argon and dye laser room to the diode testing area. This has permitted much greater availability of the argon laser and considerably increased working space near the laser beams.

e. Initial low temperature measurements on deposited junctions

During the first year of the contract, work was done on Mg-MgO-Pb, Sn-SnO-Sn and $Al\text{-}Al_2O_3\text{-}Al$ junctions. The mask described in

Section 1a was used this time except that the 5 μm wide slits were etched to a width of 50 μm. Silicon monoxide has been used particularly with Mg to slow junction change after removal from the evaporator.

Low frequency $Al-Al_2O_3-Pb$ junction second derivative $\frac{d^2 i}{dv^2}$ characteristics were recorded showing voltages of the tunneling resonances with measurement resolution better than 10 mv at liquid nitrogen and liquid helium temperatures. Comparison of liquid nitrogen traces at 10 MHz and X-band gave positions and half power line width of the 300mv resonance identical within better than 10 mv. Thus the relaxation times of these phenomena must be considerably shorter than 100 psec. Experiments were even then underway to extend these measurements to the far infrared region.

The zero-bias resonance of $Cr-Cr_2O_3-Ag$ was recorded at liquid nitrogen temperature at 10 MHz, 500 MHz and X-band. We can infer relaxation times of a fraction of a nanosecond from these data. Zero-bias anomalies over 20 percent due to impurity doping or interface defects have now been observed at liquid helium temperatures.

f. Early work on far infrared response of $Al-Al_2O_3-Pb$ junctions

Initial attempts to observe response of evaporated $Al-Al_2O_3-Pb$ at 337 μ and liquid helium were unsuccessful. In these early attempts, electrical noise from the laser made the observations difficult. Electrical shielding was then added to the HCN laser and to the critical sensor elements preparatory to looking again

for response of the junction to 337μ radiation at liquid helium temperature. Electrical noise was sufficiently reduced that observations of signals below 1 μV could be made, but laser response was not observed. Modifications were made to the laser that further improved its noise characteristics and smaller junctions were fabricated but dewar failure precluded additional runs at that time.

Later rectification characteristics of $Al\text{-}Al_2O_3\text{-}Pb$ junctions were studied at 4.2°K (liquid helium) and 2°K (helium pumped below the lambda point). In both cases the Pb was superconducting and Al was "normal." Measurements were made at 10 MHz, X-band (microwave), 337 μm (HCN laser) and with laser light in the visible.

The junctions were made by evaporating a 20 μm wide strip of aluminum to a thickness of 500 Å, oxidizing it in a few torr of pure oxygen for half an hour and then evaporating a thick 20 μm wide strip of lead across the oxidized aluminum. Resistances at 50 mV DC ranged from a few hundred to a few thousand ohms. RF was coupled to the junctions by the leads through the dewar top while the higher frequencies were beamed through the dewar windows.

In the low bias (0-20 mv) region responses to low intensity radiation of all wavelengths were the same. The superconducting transition at about 1.5 mv as well as phonon mode excitations were observed. (See Fig. 7) Widths and positions of each resonance were the same. Power saturation occurred for laser powers greater than one milliwatt. Similar saturation was observed with RF and at X-band.

At biases greater than about 20 mv and temperatures below the lambda point, tunneling resonance responses to visible laser radiation could not be detected, however there was an offset from zero which is roughly constant with bias voltage but has the same polarity as the applied bias. (See Fig. 8) Qualitatively, this response seemed to increase with increasing radiation frequency and was erroneously taken at that time as an indication of photo-response for electrons overcoming the superconducting gap. At temperatures above the lambda point, the effect of the resonances is to give a distorted bell curve. Since these observations are made with mechanically chopped radiation and amplified with coherent detection on a lock-in, this appears to be the difference between normal tunneling response at two different temperatures.

Lead on aluminum diode response to 10 MHz radiation was observed at 4.2 °K in the presence of argon laser radiation. It was observed that one mw of radiation barely reduced the structure of the 10 MHz pattern whereas 100 mw reduced it to less than 10%. Sensitivity of the response due to superconducting characteristics of lead was only slightly more reduced than the high field anomalies.

The model we currently use to explain these observations is that superfluid helium maintains the junction at nearly the same temperature, with and without radiation so that I-V curves are nearly parallel. But above the lambda point the heating causes considerable temperature rise with consequent broadening of the resonance; the lock-in displays the difference of these two curves.

Very little X-band power is coupled through the windows into the dewar. This is not enough to observe the higher bias resonances.

However, the I-V characteristics due to the superconducting gap, at about 1.5 mv are extremely sharp and make the junction a very sensitive detector; these resonances have been seen at X-band despite the very low incident power level.

Early observations indicated that the low bias (structured) signal was optimized by focusing the laser at a different point than the optimum for the offset at higher bias. Ultimately it was demonstrated that there is a definite response obtained by focusing the laser on an aluminum line which accounts for the observed offset. The junction response is restricted to the low bias region associated with tunneling between the superconductor and the normal metal. This has been quenched at fields of 1250g and partially quenched at lower fields. To determine the portion of the response which is of thermal origin, a 2500 $(\mu m)^2$ Al-Al_2O_3-Pb junction with tapered edges was fabricated. Measurements were made with a laser spot size about 20 μm diameter on the sample cooled to 1.6°K. Responses were observed for various locations on the sample as well as for different polarization orientations. A similar junction was made with a Pb disc sandwiched between thick layers of SiO, directly over the junction region. The laser light should not penetrate this shield but heat should. Behavior of the two junctions was the same indicating that the output is predominantly thermal, however, there is evidence of a small non-thermal response.

g. <u>Low temperature lead-tin junction</u>

Several low temperature runs were made with lead on tin. These very fragile junctions are easily destroyed by soldering to the substrate even with indium. Attempts to solder leads with gallium using a piece of copper wire as a soldering iron at body tempera-

ture met with limited success; gallium, just above its melting point does not wet copper or gold well. In every case, leads fell off the substrate preventing junction measurement by the time that helium was superfluid. One indium soldered junction had I-V bumps indicating a negative resistance partly shorted by junction defects (apparently induced by heating the substrate while soldering). A junction was fabricated after leads were attached to the pads and the leads later connected to the holder. The display was generally as expected, but the pattern was not sufficiently convoluted to show negative resistance.

When the Sn layers were oxidized in a glow discharge, much more stable junctions resulted than when oxidation was on a hot plate. Glow discharge time was varied, and junction resistance followed quite reproducably. Junction resistances of a few hundred ohms seemed most stable; these tolerated careful lead attachment with indium solder. Several were successfully cooled and demonstrated negative resistance characteristics in the general range of 2-3°K. (See Fig. 10) Their response to 6328 Å, 1.15 μm and RF was studied. All demonstrated rectification although response to laser radiation was predominantly thermal and quite different in character from the RF response.

h. Other superconductive work

Superconductive energy gaps were calculated at several temperatures and several combinations were found that give ratios of about two in energy at temperatures between two and four degrees K. These include Pb-V, V-Ta, V-Sn, and Pb-Sn.

Vanadium was obtained and several unsuccessful attempts were made to evaporate sufficient vanadium to make a lead on a vanadium junction. Vanadium evaporates at a considerably higher temperature than any other material we have evaporated in this laboratory. After choice of a better tungsten evaporation basket, several Pb on V samples were made, but junction resistances were not consistent; and the junctions all shorted during soldering of the leads. Since these devices should be superconducting in liquid helium without pumping, they will receive further attention.

i. Low temperature point contact

A point contact mixer assembly for adjustment and use at liquid helium temperature has been designed and fabricated. This will be used for observed mixing in the small area junctions possible with a point contact between a superconductor and a normal metal. Results will be compared with those obtained from similar "printed" structures.

SECTION 4: Optical Response

a. Mechanism of radiation detection in the visible

The response to visible radiation of a small area thin film metal-oxide-metal (MOM) structure as well as that of a mechanical metal-to-metal point contact diode, has been published.[5,6,7,8] For these, different possible mechanisms have been discussed, including optical rectification due to the nonlinear character of the electron tunneling process; this rectification process would be similar to that occurring at the infrared and the lower frequencies. The results of our experiments on high-speed (small area) thin-film vacuum-deposited junctions show that there is a significant fast response to optical frequencies arising from photoemission over the oxide's potential barrier and having the same origin as that observed sometime ago in a slow-speed, large area junction.[9] At lower frequencies, however, the mechanism must arise from a rectification process dominated by the nonlinear I-V characteristic due to electron tunneling across the junction.

In our experiment, the response of the MOM junction at room temperature to the visible radiation obtained from an argon laser is studied as a function of a bias voltage applied to the junction and the frequency of the incident radiation. Six different lines of the argon laser ranging from 4579 Å to 5145 Å are used. The measurement technique adopted in the experiment discriminates against spurious signals appearing across the junction due to thermal effects which have a long time constant (exceeding about 100 μsec). The results are then compared to the rectification of a radio-frequency signal observed in the same junction versus a bias voltage.

The studies are made on an $Al-Al_2O_3-Al$ junction, fabricated by vacuum deposition through a mechanical mask. An Al strip 20 μ wide and 1000 Å thick is first deposited and, after oxidation by exposure to ambient atmosphere for a few minutes, a similar Al strip is deposited on top of it forming with the first one a cross-like structure. The resulting impedance is in the kΩ range. The resistance of the junction depends on the thickness of the oxide layer which in turn is dependent on the method of oxidation including the temperature and length of time of exposure to oxygen. Control of the oxidation process can lower the junction impedance.

The output of the argon laser, which is tuned to operate on a single line, is focused to a spot size of 5 microns on the junction. A mechanical chopper placed at the focus of two equal achromatic confocal lenses generates 60 μsec pulses with a rise time of 2 μsec and a duty cycle of about 20. The junction response at the beginning of the laser pulse was obtained by linearly extrapolating responses taken at 10 μsec and 50 μsec respectively after the start of the pulse. A boxcar integrator with 5 μsec gate width was used to average these data. In this way, the signal across the junction due to the slow laser-induced thermal effects are subtracted. The thermal signal originates from a bolometric process which is nearly proportional to the bias voltage across the junction. In fact, this signal becomes dominant and larger than the photoemissive signal for bias voltages exceeding about 0.1 volt.

The photoemissive signal appears across the junction as a voltage pulse with a rise and decay time following that of the incident laser pulse. This signal is observed only if the laser is focused at the edge of the junction where the oxide is exposed.

The slow bolometric effect, however, is observed as long as the laser is focused on the junction or anywhere within a few microns of the junction. This effect is due to heating of the junction causing a decrease of the tunneling impedance.[10] This observation is in general agreement with the types of signals reported in Reference 11.

b. <u>Optical response of $Al\text{-}Al_2O_3\text{-}Al$ junctions</u>

The boxcar integrator procession junction response to a chopped laser signal was used to obtain Fowler plots at zero bias and for positive and negative bias levels up to 300 mV. Fowler plots at zero bias yielded barrier heights from 1.7 eV to 2.4 eV on the junctions tested, depending on the junction tested.

In one case, this barrier height was compared to that obtained from the junction resistance and the familiar Stratton formulation of tunneling current: $R_D \approx \frac{1}{162} \frac{S e^{S}}{2\phi_0 A}$

where $S = L\sqrt{\phi_0}$
L= barrier thickness in Å
ϕ_0= mean barrier height in eV
A= junction area in $(\mu)^2$

The comparison was very good, which indicates that barrier characteristics remained essentially constant from D.C. to optical frequencies, although in the former case conduction is due to tunneling, while in the latter, it is due to photoelectric effect and classical barrier penetration.

These results are included in a paper "Mechanism of Detection of Radiation in a High-Speed Metal-Metal Oxide-Metal Junction in the Visible Region and at Longer Wavelengths," by Elchinger et al., which was published in the Feb. 1976 Journal of Applied Physics. 23

The thermal response can be reduced by increasing the junction resistance, at the expense of increased junction time constant. Again, from Stratton,[10]

$$R_D(T) = R_O \frac{\sin \beta T}{\beta T}$$

where $\beta = \dfrac{\pi L k_B}{\hbar (2m/\phi_o)^{1/2}}$

T = temperature

$$\frac{\Delta R_D}{R_D} = -\frac{1}{3}(\beta T)^2 \frac{\Delta T}{T}$$

and for $T \approx 300^\circ$ K ,

$$\frac{\Delta R_D}{R_D} \approx -1.45 \times 10^{-4} \Delta T,$$

and for large R_D, ΔR will be small. Then the bolometric effect will be small for large R_D.

With the modification that junction resistance be large, either by increasing oxide thickness or decreasing junction area, it was found that photoresponse could be observed directly (without extrapolation) for zero bias and small voltages around zero bias ($\sim \pm 200$ mV).

c. Near infrared mixing experiments

Several experiments have been performed in preparation for a third order visible mixing experiment between a 1.15 μm HeNe and a dye laser at half its wavelength, using Al-Al_2O_3-Pb (Pb superconducting) junctions. The size of the desired beatnote should be the same order of magnitude as that arising from mode beating of the 1.15 μm laser itself. An early attempt to observe this mode beating was not successful. We then decided to study the system at lower frequencies and sought beatnotes from third order mix-

ing between two 9 GHz klystrons and an rf source. This observation was successful but attempts to achieve greater sensitivity by using an rf preamplifier (50 Ω input impedance) demonstrated the necessity of lowering the junction impedance to the same range. The same beatnotes have been observed, with high sensitivity, using junctions of about a hundred ohms impedance and our new low noise preamplifier. This put us in a position to re-examine the mode beating of the 1.15 μm laser. A PZT pusher was installed on this laser to facilitate continuous tuning between spatial modes separated by the measured 150 MHz when we perform the third order laser mixing.

Mixing was observed in $Al-Al_2O_3-Pb$ junctions cooled to 2.1K biased at a voltage on the order of the energy gap of Pb, e.g. ~1mV. Second order mixing involved detection of zero beat at $\nu_1 \cong \nu_2 = 9.00$ GHz. The detected signal was roughly the same magnitude as the rectified signal from either ν_1 or ν_2, which is predicted. Signals were ~40 μV pp. This beat note responded to bias in the predicted way, e.g. was zero at $V_b = 0$, maximum at $V_b \approx 1$mV, and zero at higher bias.

Third order mixing was achieved using

$$\nu_1 = 9.000 \text{ GHz}$$

$$\nu_2 = 9.100 \text{ GHz}$$

$$\nu_3 = 100 \text{ MHz}$$

The zero beat note maximized at zero bias, went through zero at V_b=1mV and had finite values for larger biases. As predicted, the zero beat showed a maximum for a specific ν_3 power.

The junction resistance at large bias was ~500Ω; at the superconducting transition, the resistance was 6000Ω. This is the "dynamic" junction resistance at the bias level which maximizes the 2nd order response.

With another junction the frequency response of a 400μm^2 area junction was tested by varying the second order beat note from zero Hz to ~200 MHz. No overall decrease in signal level was observed, although line inductance caused bands of filtering at 19 MHz, 142 MHz, and 168 MHz to occur. This response was compared to a 2500 μm^2 area junction response. Here, the junction seemed to stop responding at ~32 MHz. It was not determined whether it responds at much higher frequencies.

Second order mixing of two spatial modes of the 1.15 μm He-Ne laser was attempted using several "good" junctions. The radiation was coupled through the thin Al. However, it became apparent that with an amplifier input impedance of 50 Ω, the Al lead resistance must be very low to observe the beat signal without considerable attenuation.

A semitransparent Pb film that is electrically conducting became superconducting at 4°K. The underlying Al lead was made about 2000 Å thick. Junctions of this design have now been made with about 100 Ω junction resistance with less than 15 Ω in series. These will be used in future mixing studies.

A new detector scheme has been assembled. This incorporates a scope preamplifier and a low threshold voltage rectifier, permitting phase sensitive detection of the chopped laser signal.

A major effort is being made to observe third order mixing between a 1.15 μm He-Ne laser and a dye laser at half the wavelength. Several preparatory steps have been taken. A study of the response of Pb-Al junctions to laser radiation indicates that optical rectification contributes much of what is observed. This would imply that we have a device to perform harmonic mixing in the infrared and visible. The non-linearities of these junctions were studied by performing second and third order mixing in the microwave region with AC field strengths comparable to those available from our lasers. A Spectra Physics laser has been modified with a Smith cavity to obtain single mode 1.15 μm radiation; the other will be a dye laser at about half the wavelength. Anticipating the problem of searching for the beat note we conducted a second order mixing experiment between a single mode 6328 Å and the dye laser set to about the same wavelength. The dye laser will be roughly set with a Fabry-Perot whose mirror separation is adjustable from 0.5 mm to 5 cm so that the frequency can be tuned within 200 Mhz. Final adjustment will use a fast commercial photodiode to find a beatnote before observing it on the Pb-Al junction. Small area tunneling junctions have been studied at visible wavelengths. In particular we had expected that they could be used to mix visible and infrared radiation. A commercial HeNe laser was modified with a

Fox-Smith cavity. The laser could be made to operate at 1.15 m or 6328 Å on one or two modes. Cavity length was adjusted to give two mode output at 1.15 μm with 415 MHz spacing. Using a (thin) Al-Pb junction, the second order beat was unsuccessfully sought as was the third order by applying a 415 Mhz signal.

A tunable 6328 Å Perkin Elmer laser was beat with the Fox-Smith stabilized laser (now operated on this red line but allowed to drift thermally across the line). Tuning the Perkin Elmer laser where the other would drift through the same wavelength, a beat was observed on the Tropel detector; none could be found on a 30 KΩ Al-Pb junction.

SECTION 5: Photolithographically Defined Patterns

a. Mask fabrication

A real time V-band holographic receptor was designed, rubylith cut and sent out to be photoreduced. Masks have been made for photo production. When units were started it was discovered that there was lack of metal adherence for the lift off step. We found that glow discharge cleaning is required before metal deposition; parameters were varied and 200 μm of oxygen for 5 minutes at 2 mA seemed a good first approximation and subsequent experiments have shown this to be adequate. Time was subsequently increased to 10 minutes. Substrates must be clean, but no additional surface preparation appears necessary when the glow discharge is used.

A four element holographic sensor mask for 337 μm work has been designed and fabricated. (See Fig. 9, 1976 version)

b. Four element holographic array

Our first set of masks for the four element infrared holographic array were delivered in May 1976. Careful inspection demonstrated excellent pattern registration. The thin tips that cross to form the rectifying junctions are 2.5 μm wide, promising a potential 6.3 μm^2 junction area with perfect exposure and development. In practice these enlarge the patterns almost 1 μm in width. A metal lift process is used in which the metal is evaporated on top of a photoresist with a pattern of holes through to the substrate. When the resist is "stripped," the overlying metal is also removed. The photoresist used initially was Shipley 1350 B and later 1350 J. These are positive resists and it is the exposed areas that are subsequently taken off by the development process. Fortunately an exposed area develops its broadest opening near the substrate, thus producing an "overhang" separating the metal in the hole from

that on top of the resist and assisting in the removal of the extraneous resist and metal. Resist exposed through narrow slits in the mask will become slightly larger with overexposure, and yet an underexposed pattern may not be open completely to the substrate. Masks pick up resist from the substrate and become dirty and ultimately unusable since any cleaning process is damaging to the masks. For top quality over the whole mask, less than five exposures are usually possible. With some degradation as many as fifteen exposures are sometimes possible.

Considerable efforts were made to establish correct surface cleaning for glass and quartz substrates. Cleaning now consists of: (1) scrub surface with alkanox and water, rinse thoroughly with water and blow dry, (2) immerse for 10 minutes in chromic-sulfuric acid cleaning solution heated to about 100°C, (3) rinse in demineralized water for 3 minutes and blow dry, (4) bake 15 minutes at 185°C, and (5) cool to room temperature just before applying the photoresist. Hot nitric acid and rinse just before baking tended to make the subsequent metal deposition less adherent. Omission of the alkanox or the chromic-sulfuric caused radically reduced adherence. The bake is also essential, but excessive time again reduces adherence; this may be associated with a softening of the glass surface as indicated by ease of surface scratching with tweezers.

Initial photoresist work was done with Shipley AZ 1350 B, a thin positive resist. After conversation with the manufacturer we converted our process to AZ 1350 J which contains the same polymer, but with less solvent. The result is a thicker film giving better

separation of the film on the substrate from that on the resist. Some difficulty was experienced of erratic edge definition. So a black anodized aluminum chuck was made for the mask aligner, to prevent reflections off the chuck through the (transparent) substrate from exposing resist. This problem did not re-appear although there is reason to suspect that a more significant factor was improved technique in use of the photochemicals. The AZ 350 developer is diluted with water before use and must be thoroughly mixed (shaken) just before resist development. When this is not done considerable edge peeling occurs. In our process we find 40 second development close to optimum.

Substrate baking after development and before placing in the evaporator was tried initially, but considerable difficulty was encountered in stripping the resist. Currently we blow substrates dry and then put in the evaporator. Some experimentation was conducted to optimize time in the evaporator prior to glow discharge cleaning and evaporation, but no true optimum was found between three and twenty hours. Glow discharge is conducted in an atmosphere of 200 μm of oxygen in the valved off bell jar. A current of 2mA is run from the negatively charged aluminum discharge ring placed below the substrates. A time of 10 minutes is currently used although this does not appear critical, nor does the current. After re-pump down the chromium is evaporated.

Initially freshly broken chromium was evaporated from a tungsten basket. The chromium was quickly outgassed onto the shutter and the bell jar re-pumped before evaporation proceeded. About 300 Å of chromium are evaporated and 400 Å of nickel. More recently we have been using a chromium source plated on a piece of tungsten wire and considerably reduced substrate heating during evaporation. Excess heating during evaporation makes the resist very difficult to remove, and invariably some of the metal in the exposed areas is also removed. Attempts to increase nickel have led to poor edge definition, probably due to excess resist curing rather than the thicker metal, which is still considerably thinner than the resist. Filament-substrate distances have been adjusted to reduce heating during evaporation. It is not clear that our current eight inch spacing could not be improved.

Stripping is done in Remover 1112A at room temperature followed by a 10 minute 95°C bake before second photoresist. The second metalization is significantly different from the first in that the glass surface has now been wet without a subsequent high temperature bake. A vacuum dry or a longer pre-resist bake does not seem necessary and application will depend on the operational characteristics of the nickel oxide desired. (Fig. 11)

As in any process involving a large number of interrelated variables, the best solution generally will not be found by optimizing operations individually.

Most junctions have resistances in the desirable range of 200 to 1000Ω, and within arrays of four diodes the largest resistance is usually less than twice the smallest. In one case all four were within 12% of a mean value. About 20 μV of rectified voltage was obtained from one of the first junctions exposed to the HCN laser (337 μm).

Transfer of holographic array evaporations from the old Venco evaporation to the newer Varian was successfully accomplished late in 1976. Tightly adhering layers were deposited by avoiding overheating the substrates from the radiant evaporation source. Several excellent appearing arrays were fabricated in January 1977. Great care was used in not overheating the substrates, using fresh chromium for each evaporation and ultimately changing to the plated sources. Slightly diluted resist and making certain that samples were evaporated soon after being put in the evaporator seem to help some. Of course, great care is taken to standardize sample preparation and glow discharge cleaning. Measurements of response to the HCN laser have been made on the diodes as well as some bolometers formed by making the entire structure in one evaporation on a double exposed substrate. The best diodes had 3% coupling efficiency (comparable to what we measured on a point contact) and the response of the bolometers with optimum bias was about 1%.

These results gave promise that we could reduce the size of the diode elements and thus improve performance. Such a mask (Fig. 9 , 1977 version) was designed and held for a considerable time awaiting funds for fabrication.

SECTION 6: Point Contacts

a. Tungsten point on gold

The I-V characteristics of a tungsten point contact on gold was studied on a Tektronix 575 curve tracer for possible negative resistance.[12] Although the trace was not stable, no curve exhibited negative resistance or gaps where high speed negative resistance could have existed. In the early experiments, the contact was controlled by a micrometer, but when this adjustment proved too clumsy to achieve junction resistance over 1000 Ω, a PZT was used and resistances of several hundred kilohms were observed. Many of these traces were not stable, but none showed evidence of negative resistance at the 120 Hz trace frequency (or above). These junctions were also probed with six monochromatic visible argon laser lines. No correlation of diode output with wavelength was found.

b. Point contact antenna resistance

Measurements have been made on MOM (tungsten on nickel) point contact diodes to evaluate their effective antenna resistance as a function of length. The 10 μm diameter tungsten whisker acts as a multiwavelength antenna with effective antenna resistance of R_a. The tunneling barrier presents a junction resistance of R_d at the DC bias voltage. The point is small enough that we can neglect capacitive effects so that the voltage rectified across the diode is:

$$V_d = V_i\left(\frac{R_d}{R_a + R_d}\right)^2$$

A value of R_a can be determined by adjusting parameters on a curve of R_d vs. V_d.

A characteristic of thin dipole antennas is that the capture cross section has resonances near $n\lambda/2$ (integral values of n). The antenna resistance for very long antennas is 163 Ω.

Antenna resistances were calculated for various length whiskers with 337 μm radiation from the HCN laser. This radiation was focused onto the junction region of the diode with a teflon lens. The rectified signal was then maximized by adjusting orientation to the peak of the largest antenna lobe. R_d is varied by changing the diode contact pressure on the nickel post. To maintain a constant tunneling barrier height, all data for an R_a calculation must be taken without moving the whisker on the nickel post.

The experimental results for long antennas (longer than about 5 λ) are in agreement with the theoretical expectations ($R_a \simeq 160\ \Omega$).

Results of these measurements and those on some printed structures as well as basic calculations of MOM diode behavior are being written for publication this summer.

c. Antenna/diode calculations

Calculation of operating parameters for an infrared antenna/ diode combination has been completed. This study has been extended to include an analytical approximation of the system in closed form and evaluation or the precision of this approach. Experimental checks on the validity of our basic model are proceeding quite satisfactorily.

Previous theoretical analyses of metal-oxide-metal detectors have dealt with either the non-linearities of the junction[11,13,14] or with the antenna characteristics.[15] These theoretical results are not easily compared with measured values of detector parameters such as responsivity and noise equivalent power.

Electron tunneling across an oxide layer separating the sharply tipped tungsten wire from the (typically nickel) metal post has been recognized as the dominant (non-linear) conduction mechanism in the DC regime. It has been demonstrated experimentally that this mechanism is also responsible for rectification at least as far as the 10 μm region.[16] Devices using this principle have been used to compare harmonics of accurately known frequencies with laser sources through the infrared [17,18,19,20] and as far as 2.2 μm.[21] In practice, radiation is coupled from an electromagnetic wave to the nonlinear junction by means of an antenna that, in the case of the point contact diode, is the same tungsten wire.[22]

Our model consists of an antenna with a real internal impedance and an AC voltage source. The diode is assumed to be a non-linear resistance, calculated from tunneling theory, in parallel with a capacitance determined solely by the geometry and dielectric properties of the interfacial oxide. Computed results agree qualitatively with experiment.

A closed form approximation of the equations has been derived which permits simple evaluation of maxima knees of curves and slopes. These as well as diode NEP and rectified power correspond reasonably with computed results. The enhancement of non-linearities due to the presence of zero-bias anomalies was included in the calculations. Three orders of magnitude improvement in NEP and rectified power

are predicted at temperatures below 10°K due to the zero-bias anomalies.

A publication discussing these studies is being prepared.

d. Theoretical study of a.c. electron tunneling

A theoretical study of a.c. electron tunneling through a square barrier has been started. Its objective is calculation of the current for a Fermi distribution of electrons through a barrier whose height oscillates with a very high frequency. This is analogous to transitions in a two level system using continuous eigenstates.

The response at visible and infrared frequencies can in this way be investigated and the results compared to those obtained at dc and low frequencies. It is expected that under certain conditions, the current may have an out of phase component with respect to the applied electric field. Furthermore, these reactive components of the diodes' high frequency impedances would be non linear with respect to the applied electric field.

SECTION 7: Talks, publications and patents

a. Talks and publications

Talks by members of the group were given in Atlantic City, New Jersey (twice at the Frequency Control Symposium), La Jolla, California (Optical Electronics) and in Zurich, Switzerland (Conference on Infrared Physics). Three of these and a study of the response of metal-metal oxide-metal junctions are being published.

"High Speed Rectifying Junctions in the Infrared; Recent MIT Developments" appeared in the Proceedings of the 29th Annual Frequency Control Symposium, Atlantic City, New Jersey. It described progress in the development of metal-oxide-metal infrared diodes. Investigations have been made of the dielectric tunneling barrier formed between evaporated metallic layers and the enhancement of non-linearities by tunneling resonances. These non-linearities are a valuable spectroscopic tool and a potential means of increasing rectification efficiency. The mechanism of detection of visible radiation by a thin film MOM structure was studied. The text of this article appears as Appendix A.

"Optical Electronics: An Extension of Microwave Electronics into the Far Infrared and Infrared" is scheduled for publication in the Journal of Infrared Physics. It reviews the past activities at MIT in the area of extending frequency mixing and absolute frequency measurements in the infrared utilizing a high speed metal-metal oxide-metal junction. Recent developments in junctions deposited on a substrate are described.

Emphasis is placed on the future possibilities of large arrays and potential use as high frequency oscillators and other active elements. The text of this article appears as Appendix B.

"Mechanism of Detection of Radiation in a High-Speed Metal Oxide-Metal Junction in the Visible Region and at Longer Wavelengths" was published in the Journal of Applied Physics, February 1976[23]. It describes a study of the mechanism of detection of radiation by a small-area thin film metal-metal oxide-metal structure. After subtracting thermal effects, the response at optical frequencies is shown to arise from photoemission over the oxide's potential barrier. At lower frequencies the mechanism arises from a rectification process dictated by the nonlinear I-V characteristics due to electron tunneling across the junction. The text of this article appears as Appendix C.

"Optical Electronics, Extension of Microwave Techniques into the Optical Region" is scheduled to be published in the Proceedings of the 31st Annual Frequency Control Symposium, Atlantic City, New Jersey. It describes recent work at MIT on MOM devices evaporated through a mask or photolithographically defined as well as response of these devices to visible and infrared radiation. A study just being completed shows that a point contact MOM behaves according to classical antenna theory in the FIR. Work on printing arrays for real time holography are also described. The text of this article appears as Appendix D.

A draft of an article has been written which relates fabrication parameters to microwave/infrared behavior of MOM diodes with integral antennas. This article presents computer calculations of circuit roll-off through the infrared. The detectivity at room temperature of a single structure can be as high as 10^{10} watts $^{-1}$Hz$^{1/2}$ at frequencies of 10^{14}. As a result, design guidelines are obtained for the lithographic fabrication of thin film MOM structures that can operate to the 10 micron region of the infrared spectrum. This article will be submitted for publication soon.

b. Patents

Two patents covering optical addressing of high speed memory devices were filed with the U.S. Patent Office. They have been returned with comments. These comments were acted on and the patents refiled with slightly modified claims. Final action should be in 1977. Patents written on these concepts have also been filed in Germany and Japan as well.

Summary

Background work for this contract performed by this laboratory has shown that the tunneling characteristics of junctions formed by a very thin dielectric layer surrounded by two metals is independent of frequency (from D.C. through 10 μm wavelength). These junctions may be formed by a point contact on a lightly oxidized metal surface or by metal evaporation on such an oxidized metal surface. Work done in the initial period involved principally relatively large evaporated structures with measurements in the microwave and far infrared regions where the circuit parameters do not mask the junction characteristics. A preliminary survey of far infrared incoherent sources was conducted and such a source was procured and evaluated. The microelectronics group at Lincoln Laboratory worked on optimizing several fabrication procedures of printed structures on sapphire. Three new structures were designed and tested. Informal discussions with Perkin Elmer Optical Products Group's Research Laboratory have resulted in a plan to investigate oxide growth and characteristics of the resulting dielectric layer.

The mechanism of detection of radiation by a small area thin film metal-oxide-metal structure was studied. It was shown that after subtracting thermal effects, the response at optical frequencies arises from photoemission over the oxide's potential barrier.

Optical response of Al-Al_2O_3-Al junctions demonstrated characteristic photoemission response with considerable bolo-

metric effect. Synthesis of a model from these data showed that this model is consistent with experimental results and correctly predicts behavior at lower frequencies. A journal article based on this work was published.

Work was done on $Al\text{-}Al_2O_3\text{-}Pb$ junctions in the far infrared at liquid nitrogen and liquid helium temperatures. Interpretation of these data indicates:

a. For low non-saturating power levels at frequencies from RF through visible, junction responses at low bias (less than 20 mv) were identical.

b. For higher biases with the junction in superfluid helium, resonances were not detectable at frequencies above R.F. However, a constant offset from zero was observed (opposite senses for opposite biases) which seemed to increase with increasing radiation frequency.

c. Focusing on the Al stripe alone produced a bolometric effect. The junction gives a highly structured response only at biases less than 20 mV.

Second and third order mixing have been observed at microwave frequencies in preparation for looking at near infrared mixing. Attempts to observe second order mixing between two spatial modes of a 1.15 μm He-Ne laser were only successful after considerable work and a very small third order beat was also found. Junctions have been fabricated with a semitransparent Pb layer which became superconducting at liquid helium temperature.

Several repairs on leaks in our liquid helium dewar and one on the flexible transfer tube were done. A pump and pumping lines were installed which enable us to pump the helium in the dewar to

cool it below the lambda point and perform our experimental work in superfluid helium. A tube and mirrors were installed from the argon and dye laser room to the diode testing area. This permits greater availability of the laser and more working space near the beams.

An oxidation study was conducted on nickel which demonstrated that 400 square micrometer junctions from 100 ohms through 1 megohm can be made. These junctions are moderately stable for a few days in room ambient. Work was conducted at a very modest level over a considerable time to produce stable small area Sn-Sno-Pb junction and study their frequency characteristics. Early problems are described and ultimate success, by using a glow discharge oxidized tin layer. Attempts to evaporate V-VO_x-Pb junctions were unsuccessful due to the high evaporation temperature of V.

Real time V-band and 337 μm holographic receptors were designed and photolithographic masks made. The infrared units were built after the necessary masking and handling technologies were learned. Completed junctions were measured and are described electrically. Most good arrays are matched in resistance within a factor of two. Several mV of rectified voltage have been obtained from 5 mW incident far infrared power.

Measurements were done on MOM (tungsten on nickel) point contact diodes to evaluate their effective antenna resistance as a function of length. The effective diode resistance is varied by changing whisker pressure and response is maximized with respect to whisker orientation in the focused laser beam. Antenna resistance is obtained by adjusting parameters on a curve of diode resistance versus rectified voltage.

A mathematical model for an infrared antenna/diode combination was constructed. The expected operating parameters were calculated and a closed form analytical approximation of the theory was made with experimental checks. An article based on this work is being prepared.

A point contact mixer assembly for adjustment and use at liquid helium temperature has been designed and fabricated. Additional work was done on the I-V characteristics of a tungsten point on gold.

Four talks were given and three articles submitted for publication during this contract. Two patents covering optical addressing of high speed memory devices were filed with the U.S. Patent Office. They have since been refiled and final action is expected in 1978. Patents based on these have also been filed in Germany and Japan.

References

1. J. Giaver, Tunneling Phenomena in Solids, Edited by Burstein, Lundquist, (New York: Plenum Press), 1969. See page 21.

2. M. T. Ludwick, Indium, (New York: Indium Corporation of America), 1959, See particularly page 148.

3. D. H. Martin, Editor "Spectroscopic Techniques" North Holland Publishing Co. Amsterdam, 1967. Page 69.

4. R. C. Jacklevic and J.Lambe, Phys. Rev. Letts. 17, 1139(1966): Lambe and Jacklevic,Phys. Rev. 165, 821 (1968).

5. T. K. Gustafson, R. V. Schmidt and J. R. Perruca, Appl. Phys. Letters, 24, 620 (1974).

6. S. Faris, T. K. Gustafson and J. Wiesner, IEEE J. Quantum Elect., 9, 737, (1973).

7. S. Y. Wang, S. M. Faris, D. P. Siu, R. K. Jain and T. K. Gustafson, Appl. Phys. Letts., 25, 493 (1974).

8. Bor-long Twu and S. E. Schwarz, Appl. Phys. Letts., 25, 595 (1974).

9. A. J. Braunstein, M. Braunstein and G. S. Picus, Appl. Phys. Letts., 8 (1966).

10. R. Stratton, J. Phys. Chem. Solids, 23,1177 (1962). The tunneling conductance per unit area is $G(T) = G_o \frac{x}{\sin x}$ where $G_o = G(T=0)$ and $x = \frac{\pi LkT}{\hbar}\sqrt{\frac{2m}{\phi}} = \frac{1.023\ \pi LkT}{2\sqrt{\phi}}$ for a trapezoidal barrier model. For $x << 1$ (otherwise thermionic emission would take place rather than tunneling) we have that the corresponding resistance depends on T as

$$R(T) = \frac{1}{G(T)} = R_o \frac{\sin x}{x} \approx R_o \left(1 - \frac{x^2}{6}\right)$$

for $L = 13$ Å, $\phi = 2$ eV

and $T = 300°K$ we have $x^2 = .13$ and $\frac{\Delta R}{R} = -\frac{x^2}{3}\frac{\Delta T}{T} = -1.45 \times 10^{-4} \Delta T$

so that if $\Delta T = 70°K$, then $\frac{\Delta R}{R} \approx 10^{-2}$

11. S. J. Green, J. Appl. Phys., 42, 1166 (1971).

12. S. Y. Wang, S. M. Faris, D. P. Siu, R. K. Jain and T. K. Gustafson, Appl. Phys. Letts., 25, 493 (1974).

13. S. P. Kwok , G. J. Haddad and G. Lobov, J. Appl. Phys., 42, 554 (1971).

14. S. M. Faris, T. K. Gustafson and J. C. Wiesner, IEEE J. Quantum Elect., 7, 737, (1973).

15. C. C. Bradley and G. J. Edwards, IEEE J. Quantum Elect., 7, 548 (1973).

16. A. Sanchez, S. K. Singh and A. Javan, Appl Phys. Letters, 21, 240 (1972).

17. L. O. Hocker, A. Javan, Phys. Letters, 26A, 255 (1968).

18. V. Daneu, D. Sokoloff, A. Sanchez and A. Javan, Appl. Phys. Letters, 15, 398 (1969).

19. D. Sokolof' A. Sanchez, R. M. Osgood and A. Javan, Appl.Phys. Letters, 17, 257 (1970).

20. D. M. Evenson, J. S. Wells, F. R. Peterson, B. L. Davidson and G. W. Day, Appl. Phys. Letters, 22, 192 (1973).

21. D. A. Jennings, F. R. Peterson and K. M. Evenson, Appl. Phys. Letters, 26, 510 (1975).

22. L. Matarrese and K. M. Evenson, Appl.Phys. Letters, 17, 8 (1970).

23. G. Elchinger, A. Sanchez, C. F. Davis, Jr. and A. Javan, J. Appl. Phys. 47, 591 (1976).

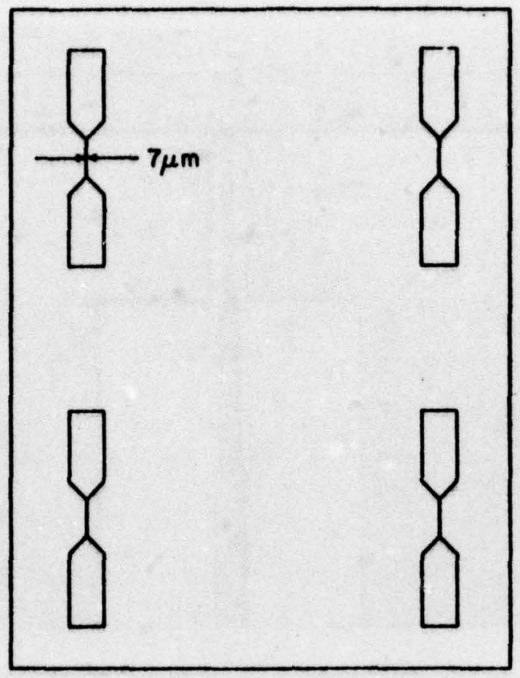

Fig. 1 Layout of Evaporation Mask

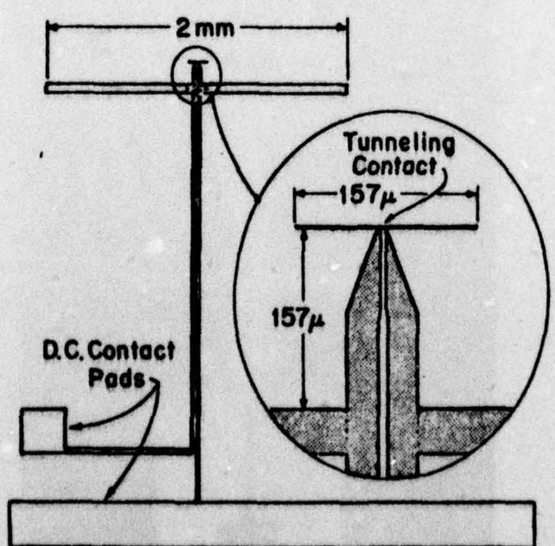

Fig. 2 Infrared and Microwave Dipoles with Tunneling Contact and DC Connections.

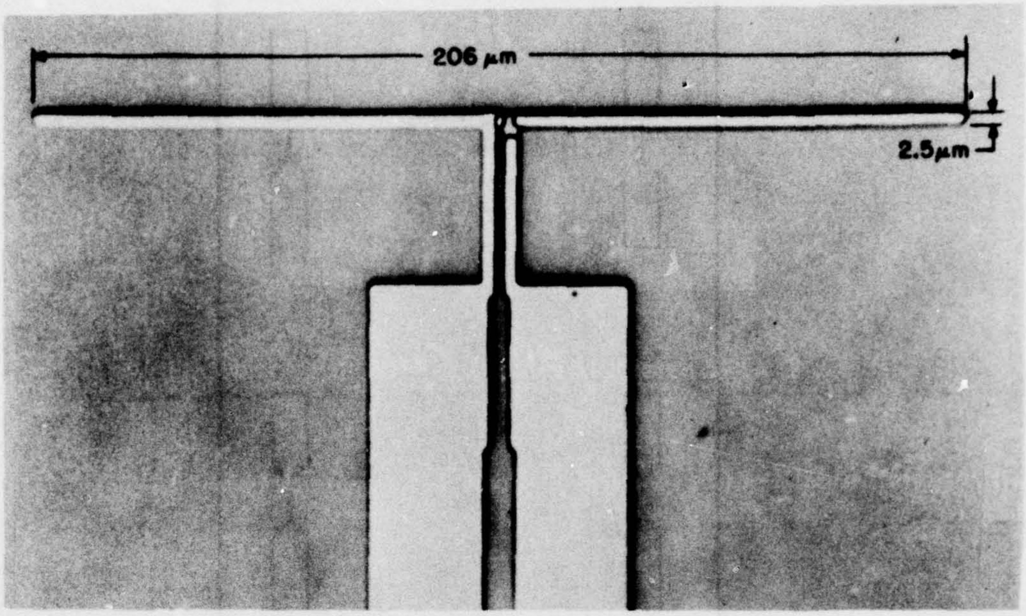

Fig. 3 $\frac{3\lambda}{2}$ Infrared Antenna. The Small Oval between the Dipole Halves is the Overlap Forming the Rectifying Junction.

Fig. 4 A Pair of $\lambda/2$ Dipoles Separated by $\lambda/2$

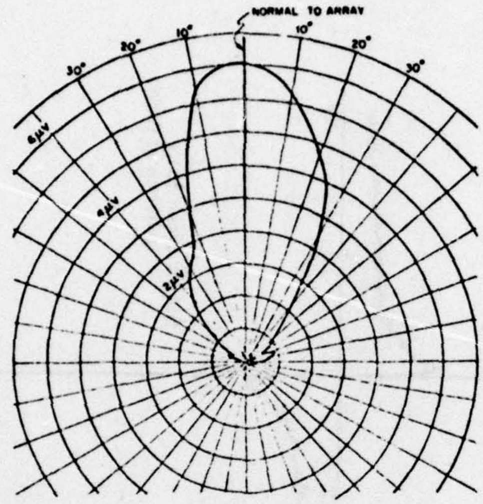

Fig. 5 Antenna Pattern of $\frac{3\lambda}{2}$ Dipole in Rotation about Dipole Feed Lines.

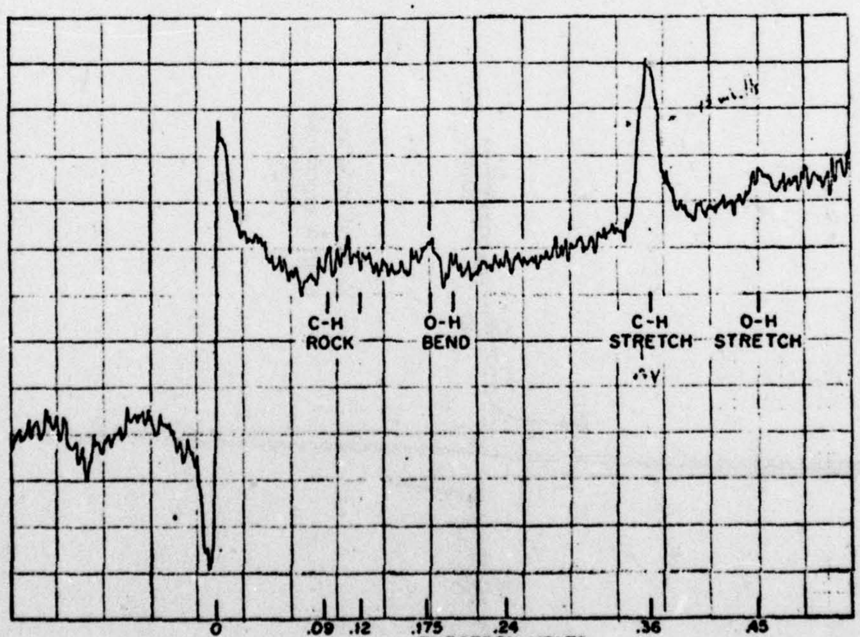

Fig. 6 Inelastic Tunneling in Aluminum - Aluminum Oxide - lead Junctions as Measured at 15 K.

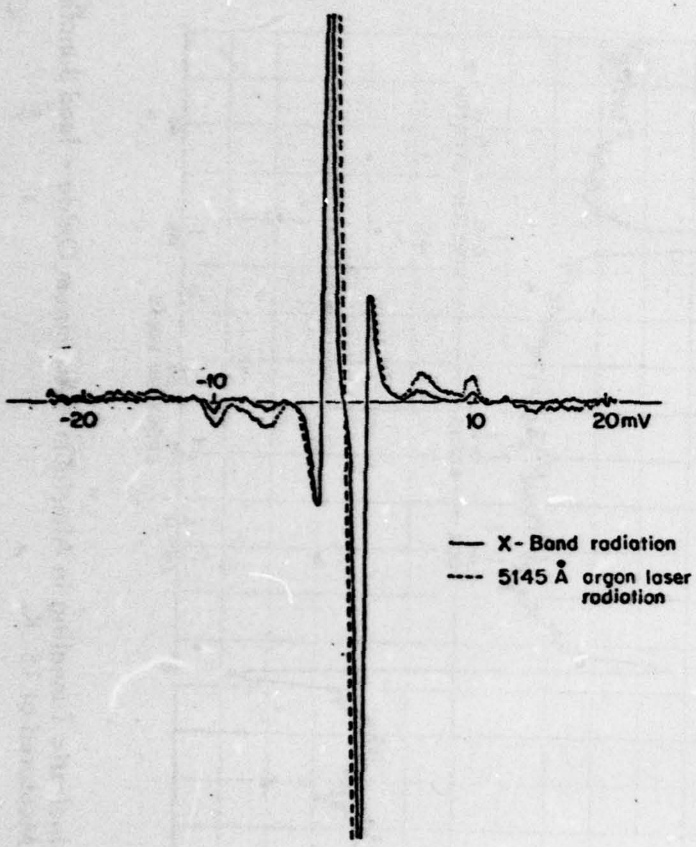

Fig. 7 Al-Al_2O_3-Pb diode responses at liquid helium temperature (2°K) in the low bias region. (0–20 mv) The argon radiation was adjusted to make first sattelite peaks of the same height. In both cases, the radiation was below saturation.

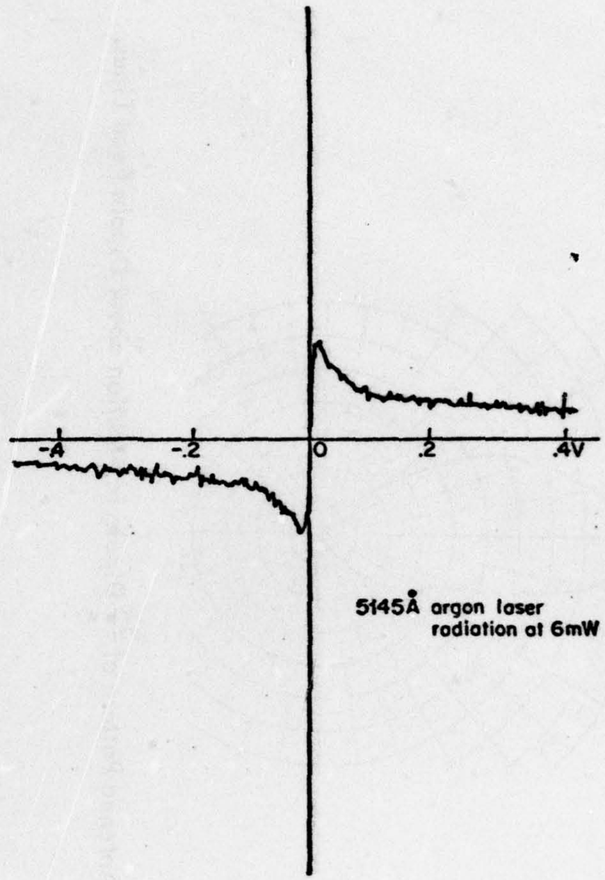

Fig. 8 Al-Al_2O_3-Pb diode responses in superfluid liquid helium at biases to $\pm 0,4$ V. The laser focus is centered on the 20 μm square junction. The vertical at zero bias is due to the superconducting transition. Note that the offset appraoches a constant value for bias greater than 0.1V.

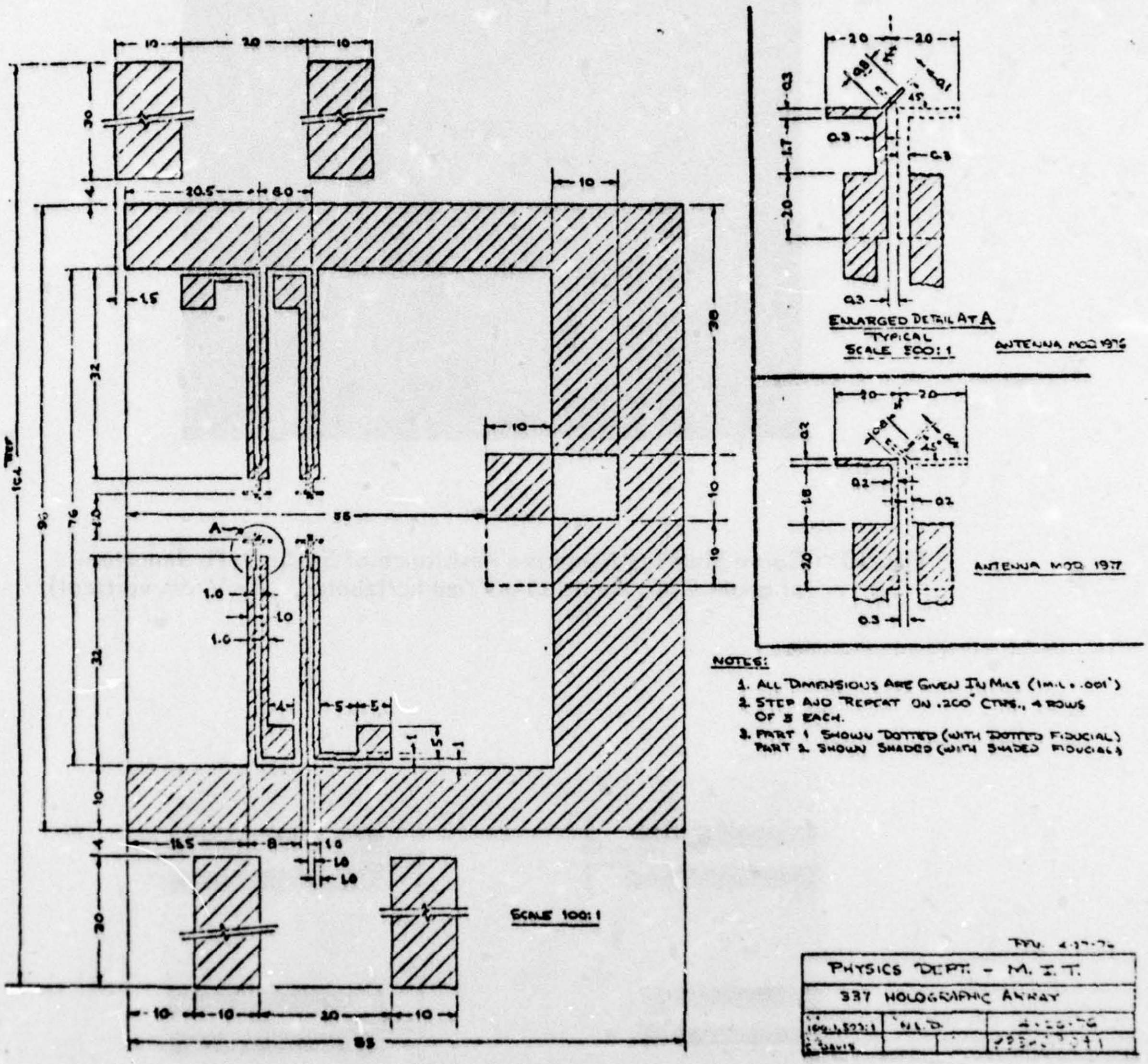

Fig. 9 Real Time Holographic Array

Fig. 10 Curve Showing Negative Resistance of Sn-SnO-Pb Junction at about 2°K. (Scale .5 mV/cm horizontal, .2 mV/cm vertical)

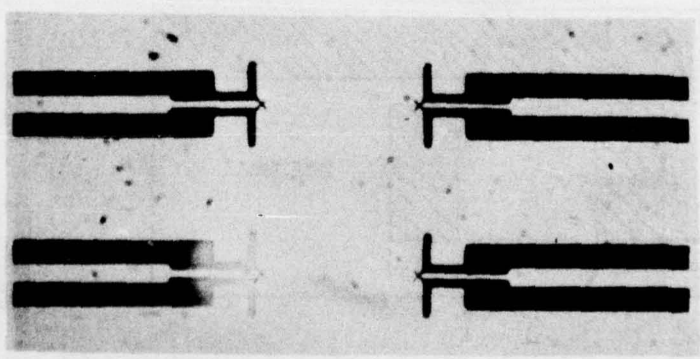

Fig. 11 Microphotograph of Diodes for Real Time Holographic Array

APPENDIX A

HIGH SPEED RECTIFYING JUNCTIONS IN THE INFRARED: RECENT M.I.T. DEVELOPMENTS*

Introduction

The extension of microwave frequency synthesis techniques to the near infrared has been made possible by the development of a metal-oxide-metal point contact diode.[1,2] Technologies have previously been described [3,4] for printing, by using evaporation and photo-lithographic processes, integral antennas with rectifier/mixer diodes; these have been applied successfully in the far infrared. Attempts to operate them at still higher frequencies require smaller RC products or greater junction non-linearities. In mixing, difference frequencies may be severely limited by the RC products. Relatively large area (tens of square microns) are currently being used to investigate the barrier form and corrections due to finite conductivity of deposited metal, large dielectric constant of the substrate, and other effects. Usable junction non-linearities, in addition to those due to the tunneling process itself, arise from paramagnetic ions and specific impurities incorporated in the dielectric.

It is also possible to obtain rectification by photoelectric emission principally from one side of a junction. In this case, coupling into the junction is no longer by antenna and wavelengths coupled to the junction are not limited by junction RC.

Dielectric Formation

Much consideration has been given to methods of insulator

* This work has been supported by Air Force-ARPA Contract No. F 19628-74-C-0182.

formation since the problems are unique when thicknesses of the order of 10 Å are required. These dielectrics of roughly 10 atom layers thickness can permit essentially no pinholes, hence self grown oxides (or possibly nitrides or sulfides) appear the most promising approach. Oxide growth on a metal is dependent on the temperature of the metal, the partial pressure of oxygen above it, possible presence of water vapor, and the permeability of the oxide to oxygen diffusion. Plasma treatment may be given to the surface to either increase or reduce oxide thickness. Insulators that are evaporated, sputtered or deposited in some other way tend to form small islands and grow to cover the surface. Such layers inherently have pinholes until their thickness is several hundred Å.

Nickel oxide was used exclusively in our early investigations because the oxide is stable at about 10 Å. In order to study some tunneling resonances, our more recent work has been done principally with non-equilibrium oxidation of freshly evaporated aluminum with controlled oxygen pressures. Non-porous layers around 10 Å thickness have been formed. Diodes made by subsequent evaporation of a second metal have been sufficiently stable in room air to make consistent measurements. The barrier energy height may vary through even a very thin oxide layer and will also depend on oxygen availability at the growing interface, thus the $Al-Al_2O_3-Al$ barrier may be asymmetric.

Tunneling Resonances

In addition to the normal electron tunneling other processes may take place. A tunneling electron may be inelastically scattered by an impurity in the dielectric;[5] the electron

loses a certain amount of energy and the impurity molecule is left in an excited state with energy $h\nu$. This process can only occur if the junction is biased with a voltage $V > h\nu/e$. As a result of this, a structure appears in the plot of $\partial^2 J/\partial V^2$ versus the bias voltage, which except for the background, is similar to the infrared spectrum of the impurity molecules in the gas phase. (See Fig. 1). Because of the thermal smearing of the Fermi level of the electodes, the use of cryogenic temperatures is necessary in order to improve the resolution of the resulting tunneling spectrum. In this way, we have observed tunneling resonances in aluminum-aluminum oxide-aluminum junctions.

This effect can be utilized in different ways. As a spectroscopic tool for chemical analysis it can give information on the impurity content of the dielectric in the tunneling junction. On the other hand, the enhanced non-linearities that result when the junctions are cooled to cryogenic temperatures will improve the performance on the MOM junctions as mixer elements.

Photoemission

The mechanism of detection of visible radiation by a thin film MOM structure[6] has been studied.[7] The response of an Al-Al_2O_3-Al junction was measured at various applied biases (to 0.3v) under irradiation successsively by six of the visible Ar laser lines. After subtracting thermal effects, the response at these optical frequencies was shown to arise from photoemission over the oxide's potential barrier, as previously demonstrated[8] in work on slow speed large area junctions. At quantum energies less than the barrier height, the detection process is dominated by rectification due to the non-linear I-V

characteristics of electron tunneling across the junction.

Conclusion

The MOM point contact diode has made possible the extension of microwave techniques into the near infrared. Printed versions of these diodes promise to have a number of advantages over the mechanical point contact diodes, including stability, reproducibility, ability to integrate antenna arrays. Much work remains to be done in understanding the details of the electron tunneling process and in searching for MOM combinations with enhanced nonlinearities. The adoption of higher resolution microelectronic techniques can be expected to yield improved device performance at the shorter wavelengths. These advances have opened the way to the exciting new field of optical electronics.

References

1. Early work in this area is reviewed by A. Javan, in Fundamental and Applied Laser Physics, Proceedings of the Esfahan Symposium, August 1971, ed. by M.S. Feld, A. Javan, and N.A.Kurnit, Wiley-Interscience, New York (1973), p. 295.
2. A. Javan and A. Sanchez in Laser Spectroscopy, Proceedings of the Vail Conference, June, 1973, ed. by R. G. Brewer and A. Mooradian, Plenum, New York, 1974, p. 11.
3. J. G. Small, G. M. Elchinger, A. Javan, A. Sanchez, F. J. Banchner and D. L. Smythe, Appl. Phys. Letts. 24, 275 (1974).
4. A. Javan and J. G. Small, in Proceedings of the 28th Frequency Control Symposium, Atlantic City, May 1974.
5. R. C. Jacklevic and J. Lambe, Phys. Rev. Letts. 17, 1139 (1966): Lambe and Jacklevic, Phys. Rev. 165, 821 (1968).

6. T. K. Gustafson, R.V. Schmidt and J. R. Perruca, Appl. Phys. Letts. 24, 620 (1974).

7. G. M. Elchinger, A. Sanchez, C. F. Davis, Jr., and A. Javan, to be published.

8. A. J. Braunstein, M. Braunstein and G. S. Picus, Appl. Phys. Letts. 8, 95 (1966).

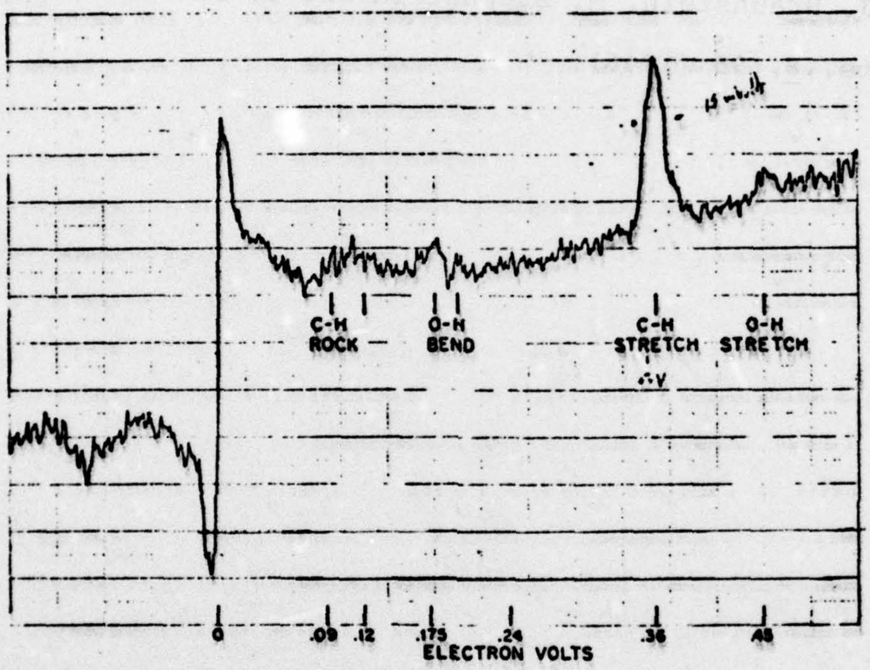

Fig. 1 Inelastic Tunneling in Al-Al_2O_3-Pb Junctions as Measured at 15 K.

APPENDIX B

OPTICAL ELECTRONICS: AN EXTENSION OF MICROWAVE ELECTRONICS INTO THE FAR INFRARED AND INFRARED

Introduction

Radio and microwave electronics is the science of electronic devices operating on the principles of alternating currents flowing through the device elements. It includes the whole technology of classical electronics composed of vacuum tubes, solid state elements, lumped or distributed elements, oscillators, amplifiers, etc.

The concepts of quantum electronics are entirely different. Electrons resonating in atoms or molecules define the device operating characteristics. These quantum mechanical principles are the basis of currently existing maser oscillators and amplifiers, quantum counters, etc.

A circuit element will allow an alternating circuit to flow through it only if its time constant is less than or comparable with the period of the alternating frequency current. The time constant is determined by the element's inherent speed and the RC time constant of the lumped circuit to which it is coupled. In most microwave electronic circuits, the overall size of the element and its associated lumped circuit components must be less than the wavelength of signal(s) it is processing. This condition avoids problems due to phase shifts which can occur over distances larger than a wavelength when current through an element runs out of phase with respect to the voltage wave. In the microwave range it is often possible to distribute components over several wavelengths and design passive elements that periodically bring current in

phase with voltage.

In quantum electronics one does not usually think in these terms; however analogies exist -- for one, an atom or a molecule's time constant is sufficiently short, allowing it to respond to frequencies where its resonances lie. As for the phase consideration, we note that this is inherently a distributed system with atoms or molecules filling volumes with dimensions of several wavelengths. The atoms keep up with the spatial phase of the electromagnetic wave, according to the laws of stimulated emission of radiation or the phase matching criteria of the parametric processes. As a result, neither the time constant nor the phase requirements have presented any problem to extension of quantum-electronic devices into the optical regions; this became a reality with the advent of lasers early in the 1960's.

Extension of radio and microwave electronics into the optical region, however, required high speed elements of microscopic size, time constants less than an optical period and dimensions less than one light wavelength. Starting in the mid-1960's, in a continuing series of efforts,[1] we succeeded in making a two-terminal high-speed junction element capable of responding at extremely high frequencies. With it we have shown that it should be possible to extend the whole science of radio and microwave electronics into the far-infrared, infrared and eventually the visible regions. All of this work is still in its infancy, but it promises to open a whole new technology which we now identify as Optical Electronics. Other approaches which can be expected to contribute to this field include MOMOM triodes, superlattice and cryogenic schottky negative resistance devices which can, in principle, operate at these frequencies and provide a whole class of active infrared devices.[2]

Point Contact Diodes

The metal-metal oxide-metal point contact diode consists of a sharply pointed wire whose tip is mechanically contacted to an oxidized flat surface. Rectification due to the non-linearities of quantum mechanical tunneling takes place at the junction which is the thin oxide layer below the sharp tip. Typically, a fifteen micrometer tungsten wire is sharpened to a point less than 1000 Å in diameter and brought into contact with a polished nickel surface that has been oxidized under ambient conditions. Studies based on tunneling theory have shown that the oxide layer is typically about 10 Å thick. Coupling of the incident infrared radiation to the junction is through the whisker which acts as a multi-wavelength antenna with the expected large number of side lobes. The detailed antenna properties can be analyzed by considering the whisker and its image, in the nickel plane, as a long wire

antenna.

It should be noted that the conductance across the junction will normally present a somewhat higher resistance than the typical 100 Ω antenna resistance. Capacitance for the assumed 10 Å thick oxide with relatively small dielectric constant will be about 10^{-14}A (where A(μm) is for example 0.01). Thus the time constant of these junctions will be about 10^{-14} seconds. This is in the range of a period of visible light. Obviously the diode mount must be rigid and offer fine adjustment of the pressure at the whisker tip. Later we will see that these same expressions govern printed circuits with junctions formed by a small metal extension overlapping an original oxidized deposit.

Frequency Multiplication in the Infrared

The effect of non-linear junction characteristics may be seen to distort the current wave when a voltage sine wave is applied. This distortion expresses itself as harmonics. For many applications the second derivative will be the most important. In much of our work higher order mixing is desirable since we mix two laser signals and a microwave signal (often harmonics of these signals) to obtain a beat signal. In this fashion harmonics of stabilized klystrons have been used to measure the frequency of a far infrared HCN laser.[3] This laser was in turn used to measure H_2O at 118μm[4] and D_2O at 84μm.[5] At the National Bureau of Standards the twelfth harmonic of the HCN laser was beat against a 28μm water vapor laser.[6] This was used to measure CO_2 laser lines[7] and finally a CO_2 harmonic was used to determine CO laser frequencies.[8] Work at the National Bureau of Standards has extended this work to the HeNe 3.39μm line[9] and the 2μm Xe line.[10]

Laser Phase Locking

A major part of our work was on developing techniques for producing a stable infrared frequency which could be phase-locked to the frequency standard. In order to compensate for laser frequency fluctuations, a microwave sideband was added to the laser frequency in the point contact diode and electrically tuned by means of a phase-locked frequency loop.[11] A harmonic of this stabilized frequency can then serve as the frequency reference in a subsequent step of the chain. In this way it is in principle possible to transfer all of the accuracy of the cesium standard to the near infrared region. In conjunction with laser frequency stabilization techniques like those described below, it is possible to conceive of new frequency standards of unsurpassed accuracy in the optical or infrared region.

The stabilization of CO_2 and N_2O lasers to the center of the Doppler profile of any of their transitions is made possible by monitoring the narrow saturation dip observed in 4.3-μm fluorescence from a low pressure absorber when a standing wave field is tuned to line center.[12] We have been studying these resonances with a view toward achieving the narrow linewidth and high signal-to-noise ratio necessary for a stable frequency or wavelength source. With the use of an expanded beam to reduce power and transit time broadening effects, and a large area He-cooled Cu:Ge detector, widths of less than 100 kHz (HWHM) have been obtained with signal-to-noise of ~200:1 at a pressure of only 1/2 mTorr.[13]

Sideband Reradiation at 10μm

An experiment has been performed at MIT which demonstrates conclusively that infrared currents do flow in antenna structures and diodes. In this experiment,[14] the point contact diode is simultaneously irradiated with monochromatic infrared radiation from a CO_2 laser and microwaves from a V-band klystron. Currents across the junction are induced at the applied infrared and microwave frequencies and as a result of the non-linearities, currents will be generated at the sum and difference frequencies (first sidebands) and to a lesser extent at other frequency combinations. The presence of currents at the first side bands is demonstrated in the experiment by heterodyne detecting the radiation coming from the point contact at the corresponding first sideband frequencies. A detailed study showed that the amplitude of the currents generated at the first sidebands has the same bias dependence as the rectified 10 μm laser radiation. Furthermore, this dependence is shown to be the second derivative of the current with respect to the voltage as obtained from the static I-V characteristic. This, in fact, is expected if the same low frequency I-V characteristic dictates the performance at frequencies as high as the infrared.

Printed Diodes

"Printed diodes" have also been made.[15] On a transparent substrate, the metallization areas are photolithographically defined and chrome overlayed with nickel is deposited. The nickel is oxidized in room air at room temperature and a second deposition is performed of nickel or gold on chrome where the chrome contacts underlying nickel oxide and acts as a glue to hold the metallization to the substrate. The nickel or gold enhances conduction. This forms the second half of the antenna structure and slightly overlaps the first deposition thereby forming the tunneling barrier diode. Comparing the antenna patterns at two HCN wavelengths shows that very considerable differences can exist over a small frequency range. These

devices have the advantage over point contact diodes of mechanical stability, reproducibility (in principle) and potentially the capability of being deposited in an array. It is possible to have arrays of several elements coupled into a single diode. One modification of the basic structure consisted of coupling a microwave and infrared dipole with the MOM diode so that the structure would be receptive to both frequencies. Mixing of a harmonic of 70 GHz with the 337 μm HCN line to yield a beat note was accomplished by this means.[15]

We feel that one unique feature of this work is realization that to function properly an infrared diode must have an extremely small cross sectional area and an extremely thin oxide. Tunneling resistance increases exponentially with dielectric thickness while capacitance goes as the reciprocal of thickness. Thus the RC product is minimized for the thinnest non porous oxide. But to retain a reasonably high resistance to avoid excessively loading the antenna, in these high speed junctions, the area must also be small. It is possible to find naturally grown oxides of the order of 10 Å thick. Nickel and tungsten form such layers at room temperature in ordinary air. Such layers can also be produced on other metals and they can be stable.

Photoemission

The response mechanism of MOM diodes has been shown to be quantum mechanical electron tunneling in the rf, microwave, submillimeter and in the infrared. But a different mechanism dominates in the visible. This is photoemission.

A study[16] was made of an Al-Al_2O_3-Al junction fabricated by vacuum deposition through a mechanical mask. The response of this junction to the radiation of six of the visible argon laser lines was measured as a function of the applied bias voltage. Spurious signals arising from long time constant (>100 μsec) thermal effects were subtracted (Fig. 1). The photoemissive signal appears across the junction as a voltage pulse with a rise and decay time following that of the incident laser pulse. This signal is observed only if the laser is focused at the edge of the junction where the oxide is exposed. The experimental results are all obtained with the power in each oscillating line set at 20 mw as measured on a calibrated power meter.

Photoemission occurs when the incident photon energy is greater than the barrier height. In the absence of bias it is known that the Al-Al_2O_3-Al barrier has an asymmetrical shape with the lower barrier height on the side of the first deposited metal.[17] When the rate of electron excitation on either side of the barrier is the

same, the net photocurrent would be zero unless the propagating electrons suffer collisions in the dielectric. After a collision the presence of the intrinsic field would favor the flow of electrons from the high side, ϕ_2, to the low side of the barrier. A net photocurrent would also result from differing rates of electron excitation on either side of the barrier. It can be shown that the photocurrent, I_{ph}, is given by $I_{ph} = A(h\nu - \phi_2)^2$ for $(h\nu - \phi_2) > kt$. Thus the voltage developed across the junction, v_s, is the product of photocurrent and tunneling impedance, R_d. Figure 2 displays the zero bias data of Fig. 1. Here $\sqrt{v_s}$ is plotted against frequency and data fit with a straight line is in excellent agreement with the photoemissive nature of the process. Intersection with the frequency axis of that straight line gives the maximum barrier height, $\phi_2 = 2.10 \pm 0.1$eV.

Inspection of the process shows that the photocurrent has a bias voltage dependence given by $I_{ph} = I_o + m V_b$, where the slope, m, is proportional to $h\nu - \phi_2$. When the experimentally determined values for the slope, m, are plotted as a function of the frequency, they fall on a straight line whose intersection with the frequency axis should, again, give the value of the barrier height ϕ_2. A value $\phi_2 = 2.12$ ev is obtained in this manner in close agreement with that reported above. Information obtained by studying the same junction at radio frequencies utilizing Stratton tunneling theory,[18] can be used to yield more information on the barrier. The measured slope of current responsivity (the ratio between the rectified current and the radiofrequency power incident on the junction) at zero bias of 2.65 volt^{-2} and the measured junction impedance of 15 KΩ make it possible to calculate a barrier height of 2.1 eV and a barrier thickness of 13Å. The value is in general agreement with experimental data[17] ($\phi = 1.77$ ev) obtained with a considerably thicker oxide formed by a different oxidation procedure.

Inelastic Scattering

Non-linearities of metal-oxide-metal diodes at room temperature can be satisfactorily understood on the basis of elastic tunneling of electrons across the potential barrier formed by the thin oxide layer. Although less likely the tunneling electron can be inelastically scattered by impurities existing in the oxide. As a result the tunneling electron gives up some of its energy and the impurity is excited to some vibrational level. If the impurity vibrational energy is $\hbar\omega_o$, the process will only have an appreciable probability if the bias voltage is $eV_b > \hbar\omega_o$. As a result it can be shown that there is step in the plot of the conductance versus bias voltage, corresponding to a change in conductance of about 1%. The second derivative $\partial^2 I/\partial V^2$ will consequently show a resonantlike structure at a voltage $eV = \hbar\omega_o$ with a width on the order of kT.

A small area, high speed junction in which inelastic tunneling takes place, would show interesting dispersive effects at frequencies in the infrared just above and below ω_o. As a result the junction would present a voltage dependent reatance at certain infrared frequencies. Such a nonlinear reactance could be utilized in some types of parametric processes and devices could be built, for example, a parametric subharmonic oscillator. This requires integrating the device to some type of resonator at infrared frequencies. Rather than using a cavity or a Fabry-Perot, smaller than a wavelength structures could be built that present a high enough Q to allow oscillations.

References

1. "Extension of Microwave Detection and Frequency Measuring Technologies into the Optical Region," A. Javan and A. Sanchez, Laser Spectroscopy, edited by Brewer and Mooradian, Page 11, Plenum Press, 1975.

2. "Tunneling in a Finite Superlattice," Appl. Phys. Letters 22, 562 (1973); "Long Journey into Tunneling," L. Esaki, Rev. of Mod. Physics 46, 237 (1974); "Electron Tunneling and Superconductivity," J. Giaver, Rev. of Mod. Physics 46, 245 (1974).

3. "Absolute Frequency Measurement of New cw HCN Submillimeter Laser Lines," L.O. Hocker and A. Javan, Phys. Letters 25A, 489 (1967).

4. "Laser Harmonic Frequency Mixing of Two Different Far IR Laser Lines up to 118 μ," L.O. Hocker and A. Javan, Phys. Letters 26A, 6 (1968).

5. "Extension of Absolute Frequency Measurement to the 84 μ Range," L.O. Hocker, J.G. Small, and A. Javan, Phys. Letters 29A, 321 (1969).

6. "Absolute Frequency Measurement of the 28 μm and 78 μm cw Water Vapor Lines," K.M. Evenson, Appl. Phys. Letters 16, 159 (1970).

7. "Extension of Laser Harmonic Frequency Mixing Techniques into the 9μ Region with an Infrared Metal Point-Contact Diode," V. Daneu, D. Sokoloff, A. Sanchez and A. Javan, Appl. Phys. Letters 15, 398 (1969); "Absolute Frequency Measurement of the CO_2 cw Laser at 28 THz (10.61 μm)," K.M. Evenson, J.S. Wells and L.M. Matarrese, Appl. Phys. Letters 16, 251, (1970).

8. "Extension of Laser Harmonic Frequency Mixing into the 5μ Region," D. Sokoloff, A. Sanchez, R. Osgood, A. Javan, Appl. Phys. Letters 17, 257 (1970).

9. "Accurate Frequencies of Molecular Transitions Used in Laser Stabilization: the 3.39 μm Transition in CH_4 and and the 9.33 and 10.18 μm Transitions in CO_2," K.M. Evenson, J.S. Wells, F.R. Petterson, B.L. Danielson and G.W. Day, Appl. Phys. Lett. 22, 192 (1973).

10. "Extension of Absolute Frequency Measurements to 148 THz: Frequencies of the 2.0 - and 3.5-μm Xe Laser," D.A. Jennings, F.R. Petersen and K.M. Evenson, Appl. Phys. Letters, 26, 510 (1975).

11. "Precision Absolute Frequency and Wavelength Measurements in the Infrared: A Review of Activities at MIT," J.G. Small, J.-P. Monchalin, M.J. Kelly, F. Keilmann, A. Sanchez, S.K. Singh, N.A. Kurnit, A. Javan, and F. Zernike, Proceedings of the 26th Annual Frequency Control Symposium, Atlantic City, June 1972.

12. "Standing Wave Saturation Resonances in the CO_2 10.6μ Transitions Observed in a Low Pressure Room Temperature Absorber Gas," C. Freed and A. Javan, Appl. Phys. Letters 17, 53 (1970).

13. "Potential Frequency Accuracy of the CO_2 Fluorescence Saturation Dip," M.J. Kelly, J.E. Thomas, J.-P Monchalin, N.A. Kurnit, and A. Javan, Proceedings of the 29th Annual Frequency Control Symposium, Atlantic City, May, 1975 (in press).

14. "Generation of Infrared Radiation in a Metal-to-Metal Point Contact Diode at Synthesized Frequencies of Incident Fields; A New High Speed Borad Band Light Modulator," A. Sanchez, S.K. Singh and A. Javan, Appl. Phys. Letters 21, 240 (1970).

15. "A.C. Electron Tunneling at Infrared Frequencies; A Thin Film M-O-M Diode Structure with Broad-Band Characteristics," J.G. Small, G.M. Elchinger, A. Javan, A. Sanchez, F.J. Bachner, and D.L. Smythe, Appl. Phys. Letters 24, 275 (1974).

16. "Mechanism of Detection of Radiation in a High-Speed Metal-Metal Oxide-Metal Junction in the Visible and Radiofrequency Regions," G.M. Elchinger, A. Sanchez, C.F. Davis, Jr., and A. Javan, to be published.

17. "Voltage Dependence of the Barrier Heights in Al_2O_3 Tunnel Junctions," A.J. Braunstein, M. Braunstein and G.S. Picus, Appl. Phys. Letters 8, 95 (1966).

18. "Volt-Current Characteristics for Tunneling Through Insulating Films," R. Stratton, J. Phys. Chem. Solids 23, 1177 (1962).

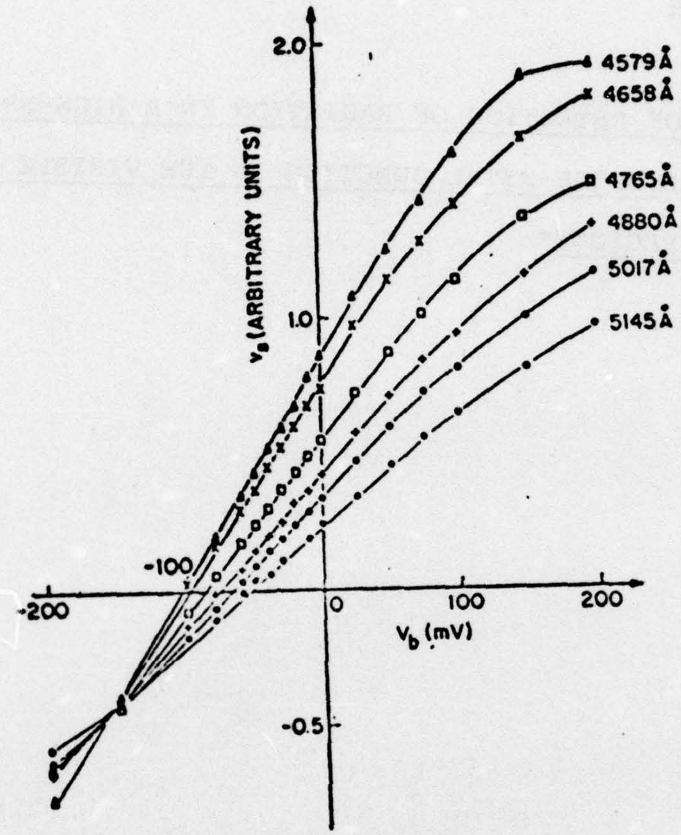

Figure 1. Photoresponse of small area Al-Al_2O_3-Al junction versus applied bias voltage at different wavelength radiations. For $(h\nu - \phi_2) > kT$, $(h\nu - \phi_2) \propto I_{ph}$, as shown in Fig. 2.

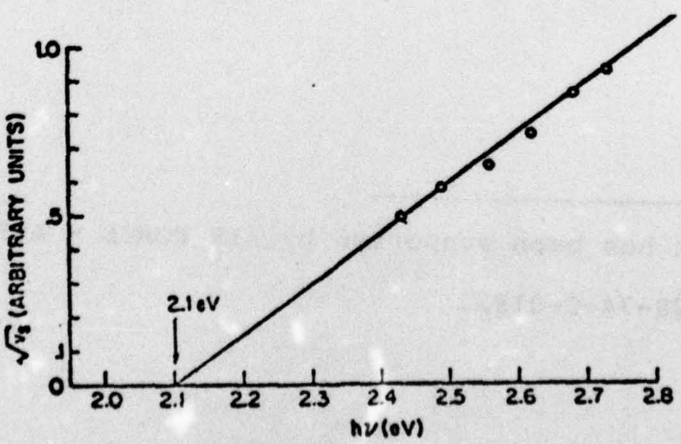

Figure 2. Fowler plot of zero bias data from Fig. 1. Square root of the response voltage is plotted against photon energy and best straight line is drawn through the data. The zero response value is the barrier height.

APPENDIX C

MECHANISM OF DETECTION OF RADIATION IN A HIGH-SPEED METAL-METAL OXIDE-METAL JUNCTION IN THE VISIBLE AND RADIO-FREQUENCY REGIONS*

* This work has been supported by AIR FORCE - ARPA Contract No. F19628-74-C-0182.

The response to visible radiation of a small area thin film metal-oxide-metal (MOM) structure as well as that of a mechanical metal-to-metal point contact diode, has been previously reported.[1-4] For these, different possible mechanisms have been discussed, including optical rectification due to the nonlinear character of the electron tunneling process; this rectification process would be similar to that occurring at the infrared and the lower frequencies. This letter gives the results of an experiment in a high speed (small area) thin film deposited junction which shows that the response to optical frequencies arises from photoemission over the oxide's potential barrier and has the same origin as that observed sometime ago in a slow speed, large area junction.[5] At lower frequencies, however, the mechanism is shown to arise from a rectification process dictated by the nonlinear I-V characteristic due to electron tunneling across the junction. This letter also gives new information on the photoemission process, not previously reported.

In the experiment, the response of the MOM junction at room temperature to the visible radiation obtained from an argon laser is studied as a function of a bias voltage applied to the junction and the frequency of the incident radiation. Nine different lines of the argon laser ranging from 4579Å to 5145Å are used. The measurement technique adopted in the experiment discriminates against spurious

signals appearing across the junction due to thermal effects which have a long time constant (exceeding about 100 μsec). The results are then compared to the rectification of a radio frequency signal observed in the same junction versus a bias voltage. The barrier parameters obtained from photo-emission theory applied to the visible radiation response are found to be in excellent agreement with the parameters obtained from electron tunneling giving rise to the nonlinear I-V characteristic responsible for the rectification of the radiofrequency signal.

The studies are made in an $Al-Al_2O_3-Al$ evaporated junction, fabricated by vacuum deposition through a mechanical mask. An Al strip 20μ wide and 1000Å thick is first deposited and, after oxidation by exposure to ambient atmosphere for a a few minutes, a similar Al strip is deposited forming with the first one a cross-like structure. The resulting impedance is in the kΩ range.[6]

In the experiment the output of the argon laser oscillating in a single line is focused onto the junction with a spot size of 5 microns. A mechanical chopper placed at the focus of two equal achromatic confocal lenses generates 60 μsec pulses with a rise time of 2 μsec and a duty cycle of about 20. The voltage appearing on the junction due to the laser pulse is averaged with a boxcar integrator at two times during the pulse and extrapolated back to the beginning of the pulse . In this way the signal across the junction due to the slow laser-induced thermal effects are subtracted. The

thermal signal originates from a bolometric process which is nearly proportional to the bias voltage across the junction. In fact, this signal becomes dominant and larger than the photoemissive signal for bias voltages exceeding about .1 volt.

The photoemissive signal appears across the junction as a voltage pulse with a rise and decay time following that of the incident laser pulse. This signal is observed only if the laser is focused at the edge of the junction where the oxide is exposed. The slow bolometric effect, however, is observed as long as the laser is focused on the junction or anywhere within a few microns of the junction. This effect is due to heating of the junction causing a decrease of the tunneling impedance.[7] This observation is in general agreement with the types of signals reported in Ref. 1.

The experimental results reported below for six different laser lines are all obtained with the power in each oscillating laser line attenuated to the same power level, 20 mw, as measured with a calibrated power meter.

The experimental results are presented in Fig. 1a where the detected voltage, v_s, is plotted for a given frequency, as a function of the bias voltage. This family of curves also gives the response versus the frequency at various bias voltages, V_b, and contains information on the mechanism occurring in the junction.

The photoemission process occurs when the incident photon energy is higher than the barrier height. In this case the electrons in the metal on each side of the barrier are excited to an energy above the top of the barrier. The excited electrons can then propagate across the barrier in either direction. Consider first the photoemission process in the absence of an applied bias voltage. For an $Al\text{-}Al_2O_3\text{-}Al$ junction, it is known that the barrier has an asymetrical shape with the lower barrier height on the side of the first deposited metal (see barrier shape in Fig. 2).[5] It is also known that for the case where the rate of electron excitation on either side of the barrier is the same, the net photocurrent would be zero unless the propagating electrons suffer collisions in the dielectric. After a collision the presence of the intrinsic field would favor the flow of electrons from the high side to the low side of the barrier. It is also to be noted that a net photocurrent would result if the rate of electron excitation differs on either side of the barrier. For both cases it can be shown that the photocurrent, I_{ph}, is given by $I_{ph} = A(h\nu - \phi_2)^2$. This formula holds when $h\nu - \phi_2 \gg kT$. Accordingly, the voltage developed across the junction, v_s, would be the product of the photocurrent times the tunneling impedance, R_d.

Figure 1b displays the data in Fig. 1a for zero bias ($V_b = 0$). In this figure, $\sqrt{v_s}$ is plotted versus frequency. The fit of the data with a straight line is in excellent

agreement with the photoemissive nature of the process. The intersection with the frequency axis gives the maximum barrier height $\phi_2 = 2.10 \pm 0.1$ eV

The above behavior is similar to that observed in large area junctions in which the second deposited metal was sufficiently thin to allow the applied radiation to penetrate through the thickness of the metal. In that experiment[5] the measured maximum barrier height, ϕ_2 , for an Al-Al_2O_3-Al junction was 1.77eV. The difference we attribute to different oxidation procedure.

The slopes of the curves presented in Fig. 1a can also be used to obtain a precise measure of the barrier height; it can be shown that in the presence of a small bias voltage, the contribution to the net photocurrent from photoelectrons originated in side 1 (see Fig. 2) is changed while that from side 2 remains essentially unaffected. As a result, the photocurrent has a bias dependence that in the first approximation is linear and given by $I_{ph} = I_o + mV_b$ where $m \propto (h\nu - \phi_2)$. Figure 1c displays the slope, m, versus $h\nu$ as obtained from the data points given in Fig. 1a. Notice that the intersection with the frequency axis gives again a measure of the barrier height $\phi_2 = 2.12 \pm 0.1$eV in excellent agreement with the above results. This effect has not been reported previously and is highly useful for determining barrier height.

The curvature of the curves in Fig. 1a arises in part from the decrease in the tunneling impedance as a function of current. Furthermore, at higher voltages the lowering of the barrier height becomes an appreciable effect and contributes to the observed curvatures. Inspection of the data in Fig. 1a for large bias voltages is in general agreement with this effect.[8]

The response of a small area deposited metal-oxide-metal junction to infrared radiation has recently been observed and shown to be the same as the response obtained in the far infrared, microwaves or the radiofrequency regions.[9] This arises from the rectification process predicted by the nonlinear I-V characteristic of the junction. For a junction of the dimensions used in this experiment, the capacitance is sufficiently low to allow appreciable coupling of the junction to a radiofrequency or microwave signal. The current responsivity, β_i , defined as the ratio between the rectified current, i_r, and the radiofrequency power, P, coupled to the junction ($\beta_i = i_r/P$) is determined by the local value of the second derivative of the junction's I-V characteristic at the point of operation ($\beta_i = \frac{1}{2} \left.\frac{\partial^2 I}{\partial V^2}\right|_{V_b} R_d$ where R_d = junction's resistance). Figure 3, therefore, displays the current responsivity versus the

applied bias voltage, V_b. For the above junction, the measured βi for $V_b = 0$ is 0.087 volt^{-1} for a measured junction impedance of $R = 15k\Omega$.

In the same manner that has been shown for mechanical metal-to-metal point contact diodes[10], it is possible to obtain the potential barrier parameters from the above measurements by direct application of the results of the electron tunneling theory. It can be shown[7] and is in agreement with the experimental results that for small bias voltages the junction's responsivity has a linear dependence on the bias voltage given by $\beta_i = \beta_i(V_b = 0) + u V_b$. From Fig. 3 we find that $u =$ 2.65 volt^{-2}. From the tunneling theory u and R_d are found to be functions of the average barrier height, ϕ_o, and thickness, L given by $u = \frac{1}{2}(S/4\phi_o)^2$ and $R_d = S e^S/(320\,\phi_o a)$. The junction's area, a, is given in (microns^2), R_d in ohms and S is a dimensionless parameter given by $S = 1.02L\sqrt{\phi_o}$ with L in angstroms and ϕ_o in electron volts. Solution of the above equations using our measured values: $u = 2.65$ volt^{-2} and $R_d = 15k\Omega$ gives: $\phi_o = 2.1$eV and $L = 13$Å. Note the agreement between this value of the barrier height and that obtained from measurement at optical frequencies.

The above agreement between the measured values of the barrier height is a striking demonstration that the same potential barrier that determines the properties of the junction at a radiofrequency also determines the behavior at optical frequencies. These properties arise from related, thought different, types of quantum mechanical processes.

In the case where the frequency of the applied radiation is comparable to the barrier height, the contribution to the photocurrent due to photon assisted tunneling can become quite important. It can be shown that, even in the present work in which $h\nu - \phi_2$ was about 0.5eV the contribution due to photoelectrons with energies below the top of the barrier amounts to 5 to 10% of the total photocurrent. These and other related details will be published separately.

REFERENCES

1. T. K. Gustafson, R. V. Schmidt and J. R. Perruca, Appl. Phys. Letters 24, 620 (1974).

2. S. Faris, T. K. Gustafson and J. Wiesner, IEEE J. Quantum Electron. QE-9 737 (1973).

3. S. Y. Wang, S. M. Faris, D. P. Siu, R. K. Jain and T. K. Gustafson, Appl. Phys. Letters 25, 493 (1974).

4. Bor-long Twu and S. E. Schwarz, Appl. Phys. Letters 25, 595 (1974).

5. A. J. Braunstein, M. Braunstein and G. S. Picus, Appl. Phys. Letters 8, 95 (1966).

6. The resistance of the junction depends on the thickness of the oxide layer which in turn is dependent on the method of oxidation including the temperature and length of time of exposure to oxygen. Controlled oxidation process can be used to obtain lower impedance.

7. R. Stratton, J. Phys. Chem. Solids 23, 1177 (1962).

   The tunneling conductance per unit area is $G(T) = G_o \frac{x}{\sin x}$ where $G_o = G(T=0)$ and $x = \frac{\pi}{2} \frac{L}{\sqrt{\phi}} kT$ for a trapezoidal barrier model. For $x \ll 1$ (otherwise thermionic emission would take place rather than tunneling) we have that the corresponding resistance depends on T as

   $$R(T) = \frac{1}{G(T)} = R_o \frac{\sin x}{x} \approx R_o \left(1 - \frac{x^2}{6}\right)$$

   for $L = 13\,\text{Å}$, $\phi = 2\,eV$

   and $T = 300°K$ we have $x^2 = .13$ and $\frac{\Delta R}{R} = -\frac{x^2}{3}\frac{\Delta T}{T} = -1.45 \times 10^{-4} \Delta T$

   so that if $\Delta T = 70°K$, then $\frac{\Delta R}{R} \approx 10^{-2}$

8. A detailed analysis of this effect will be presented in a subsequent publication.

9. J. G. Small, G. M. Elchinger, A. Javan, A. Sanchez, F. J. Bachner, D. L. Smythe, Appl. Phys. Letters 24, 275 (1974).

10. A. Javan and A. Sanchez, Laser Spectroscopy, proceedings of the Vail Symposium p. 11, edited by R. G. Brewer and A. Mooradian, Plenum Press (1974).

FIGURE CAPTIONS

Figure 1. (a) Photoresponse of small area $Al-Al_2O_3-Al$ junction versus applied bias voltage at different wavelength radiations. For $(h\nu - \phi_2) \gg kT$, $(h\nu - \phi_2) \propto \sqrt{I_{ph}}$, as shown in (b). These points are taken from (a) at $V_b = 0$. (c) shows the linear behavior of the slope of I_{ph} versus incident photon energy around zero bias. This indicates that for small applied bias voltage, the net change in the photocurrent is a linear function of V_b.

Figure 2. (a) Potential barrier shape at zero bias modeled from a basic trapezoid. Electrodes 1 and 2 are the first and second deposited Al strips, respectively. ϕ_2 is the larger barrier potential as determined experimentally. (b) Barrier altered by applied (positive) bias on electrode 1. At $T \approx 0°K$, the maximum photoexcited electron energy will be $h\nu$ above each Fermi level.

Figure 3. Display of the current responsivity, β_i, versus applied bias voltage, V_b. By definition $\beta_i = i_r/P$ where P is the radiofrequency power coupled to the diode and is given by $P = \frac{v_{rf}^2}{R_d}$. Therefore $\beta_i = \frac{v_r}{v_{rf}^2}$ and is determined from the experiment by measuring the coupled radiofrequency voltage, v_{rf}, (r.m.s. value) and the resulting rectified voltage, v_r.

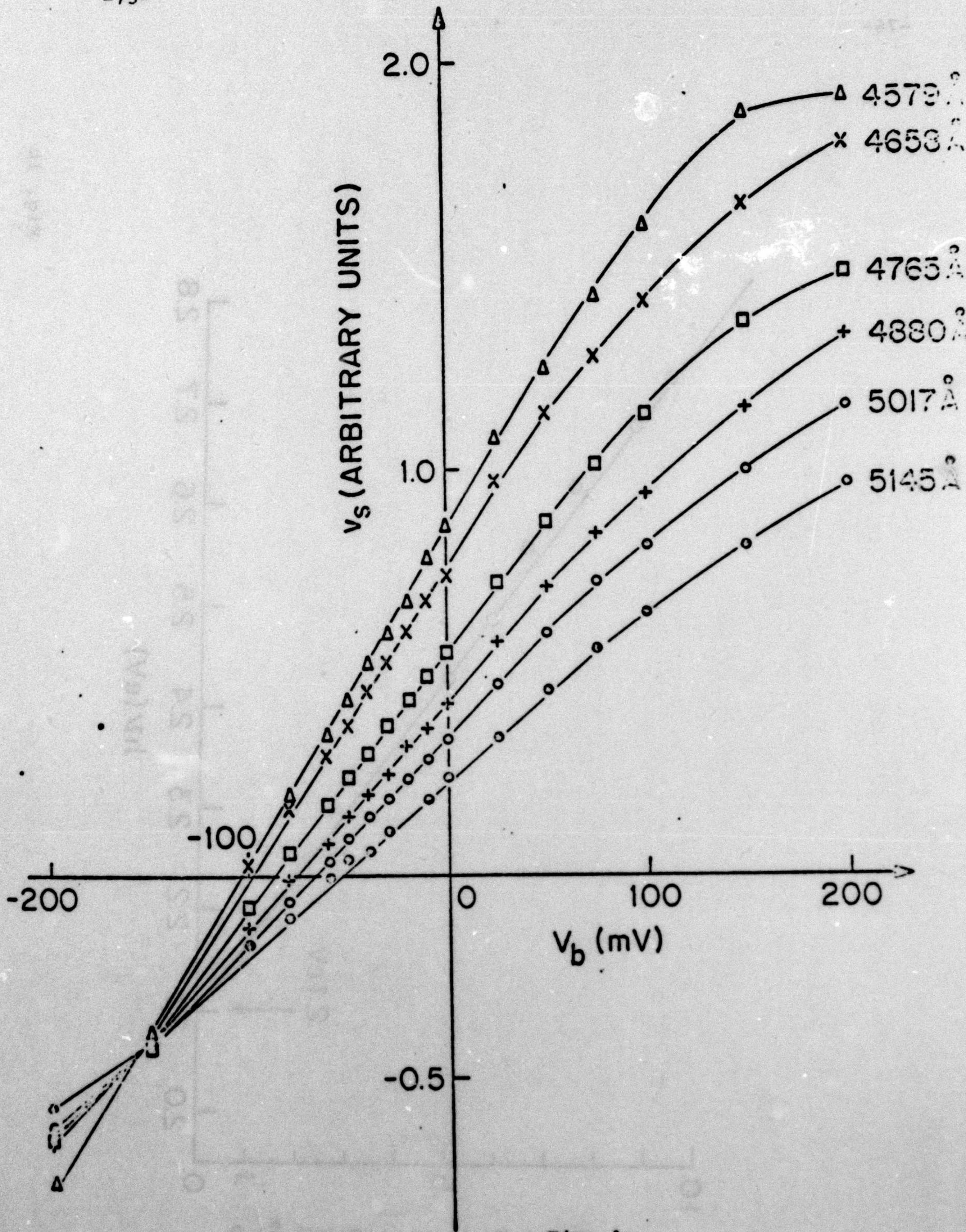
2.0
1.0
-0.5
-100
-200
0
100
200
v_s (ARBITRARY UNITS)
V_b (mV)
4579 Å
4658 Å
4765 Å
4880 Å
5017 Å
5145 Å

Fig. 1a

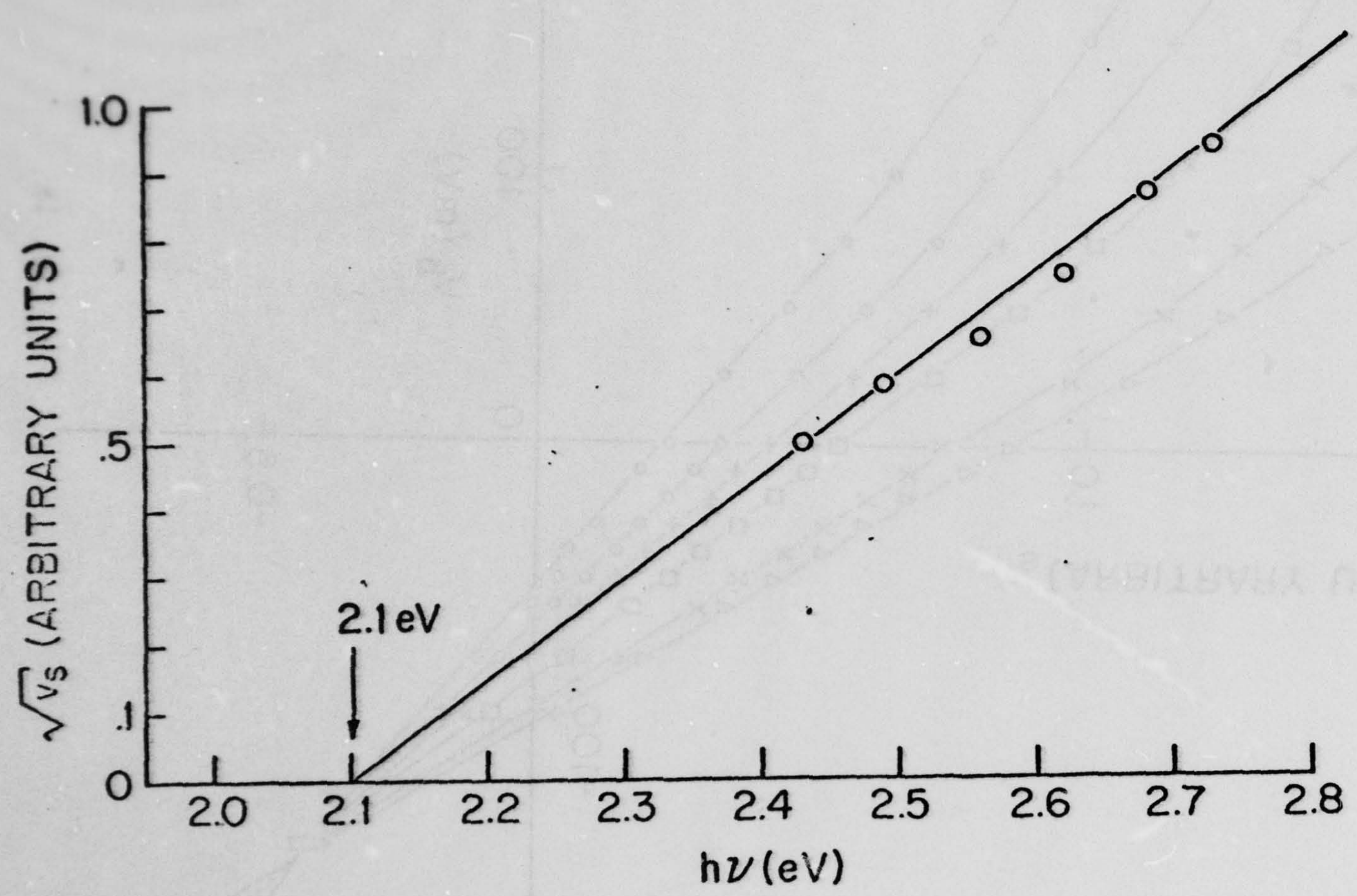

1.0
.5
.1
0
$\sqrt{V_S}$ (ARBITRARY UNITS)
2.1eV
2.0
2.1
2.2
2.3
2.4
2.5
2.6
2.7
2.8
$h\nu$(eV)

Fig. 1b

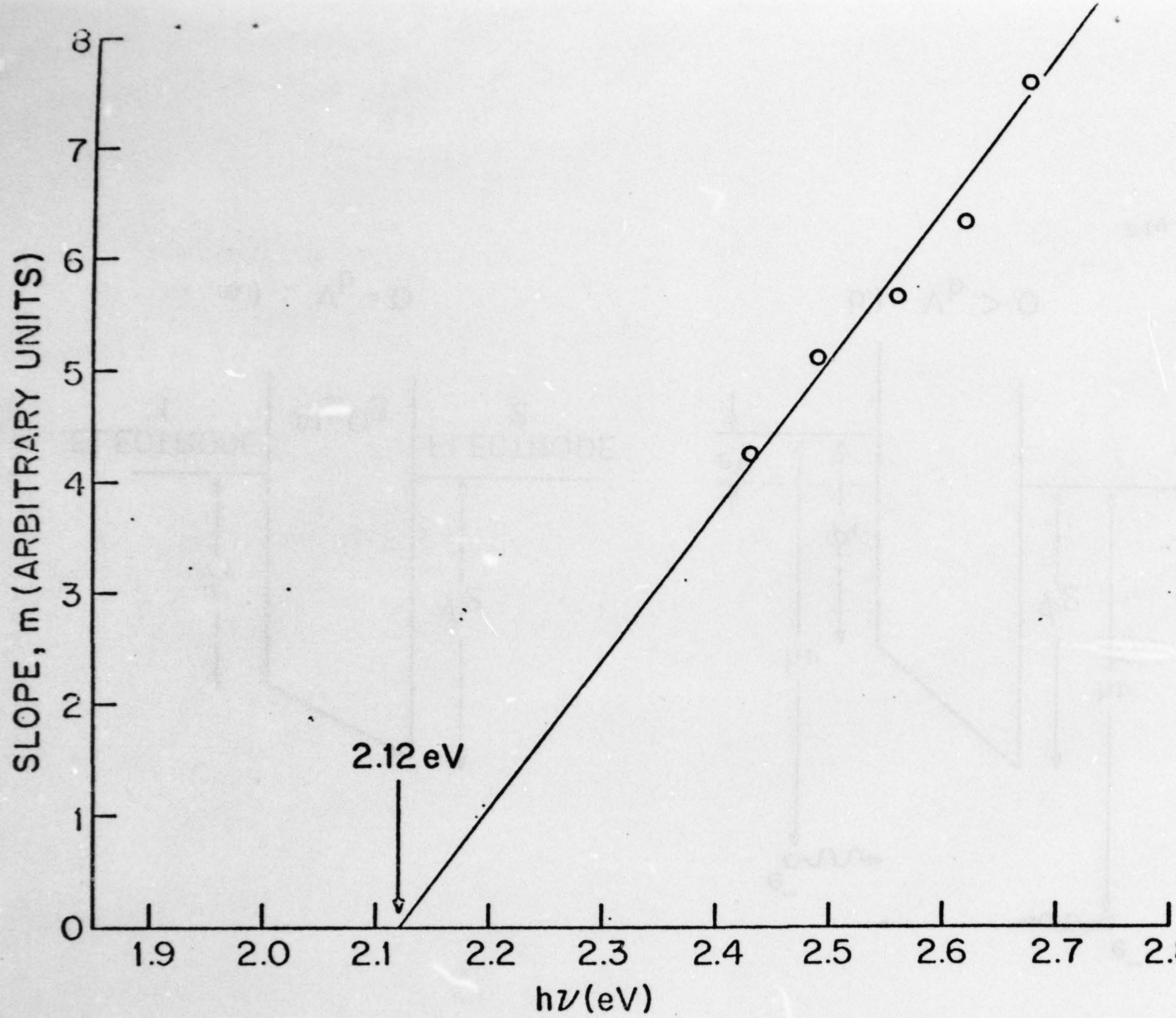

SLOPE, m (ARBITRARY UNITS)
0
1
2
3
4
5
6
7
8
2.12 eV
1.9
2.0
2.1
2.2
2.3
2.4
2.5
2.6
2.7
2.8
hν(eV)

Fig. 1c

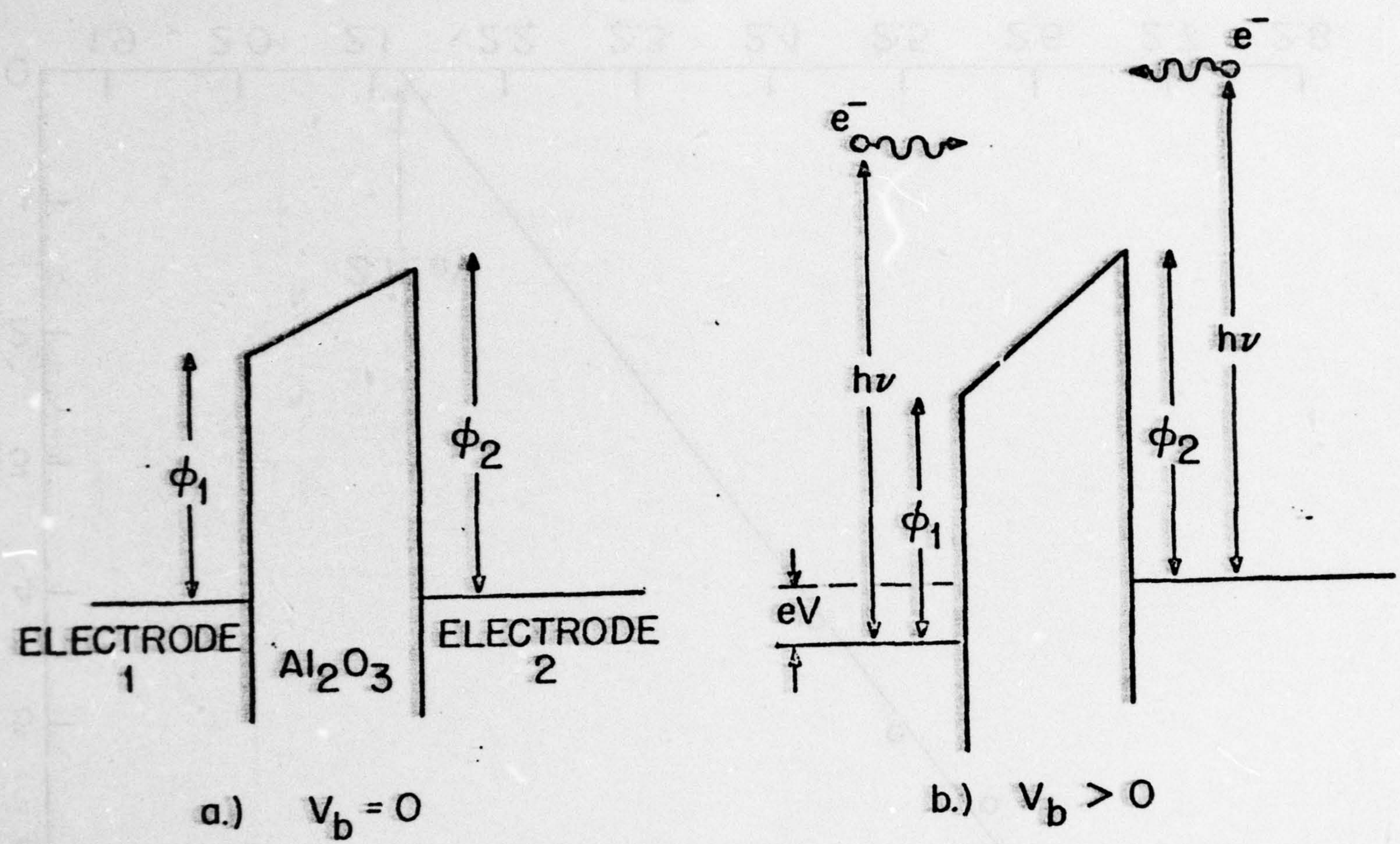

Fig. 2

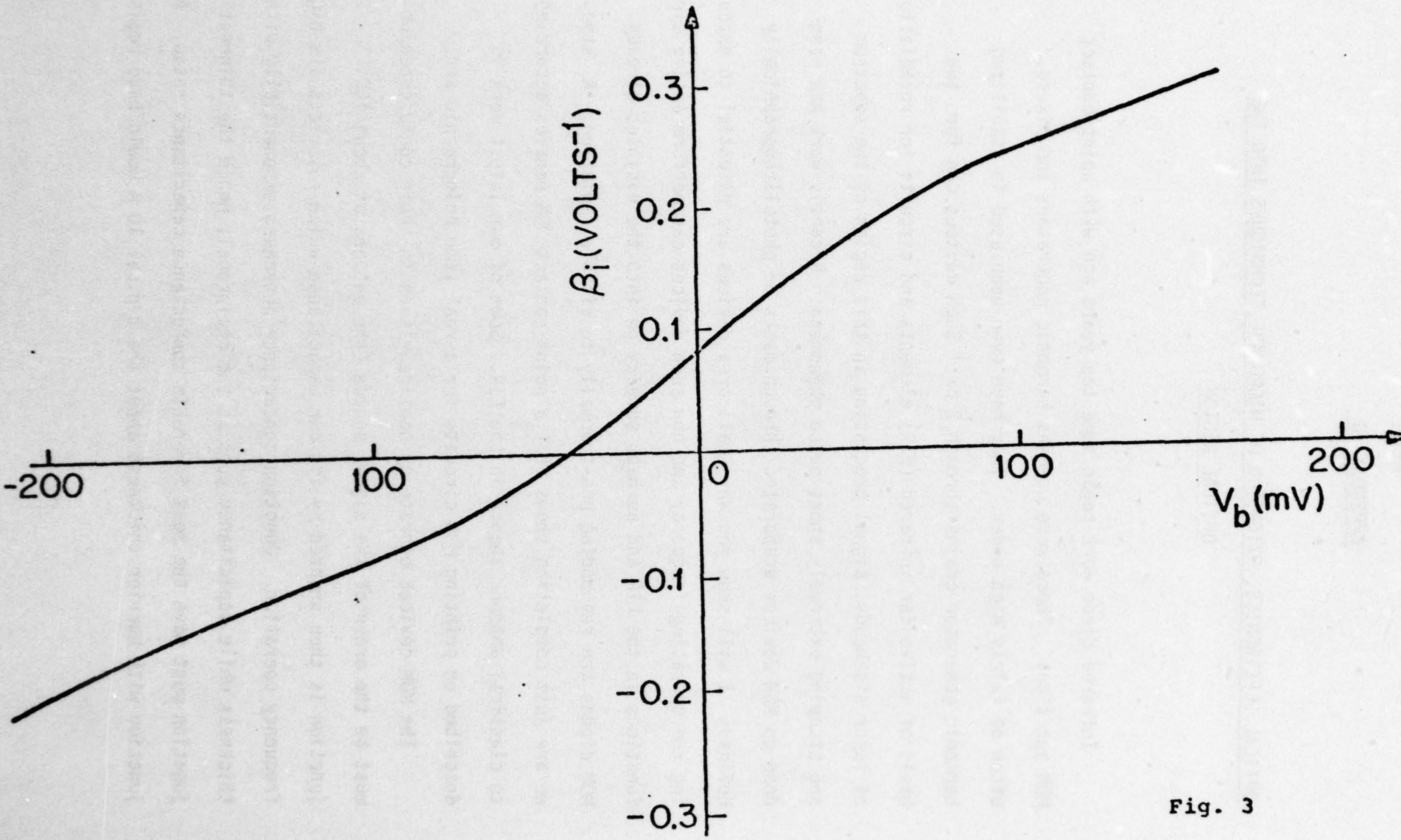

Fig. 3

APPENDIX D

OPTICAL ELECTRONICS, EXTENSION OF MICROWAVE TECHNIQUES INTO THE OPTICAL REGION

Infrared diode work began some ten years ago with point contact MOM junctions. These were used as harmonic generators and mixers, often of fairly high order. They have even been used in stabilized harmonic generator chains through 2 μm.[1] Such devices can form the basis of active far infrared (FIR) elements and circuits for reradiation of laser sidebands, signal processing in this region of the spectrum and studying extremely short pulse phenomena. Recently work has been done on MOM devices evaporated through masks or photolithographically defined. I will show you why small area devices are essential to extending the operating frequency and how such devices can perform active circuit functions in the FIR and perhaps someday on into the visible; already MOM diodes are responding non-thermally to visible radiation. A study we are just completing shows that a point contact MOM behaves according to classical antenna theory in the FIR. Some of our latest work is described on printing MOM circuits for a real time holographic array.

The MOM devices operate by nonlinearities in their conductance, which must be the order of the signal source (the antenna at about 100 Ω). This junction is then shunted by its own capacitance which restricts its high frequency operation. Junction conductance decreases exponentially with thickness while capacitance goes as the reciprocal; hence the thinnest junction must have the most favorable conductance capacitance ratio. A junction with barrier thickness about the typical 10 Å would have resis-

tance of $10^2\ \Omega/A$ (A in μm^2) requiring about 1 μm^2 to match the typical antenna/resistance. Orders of magnitude change in the area can be compensated for by small changes in barrier thickness to maintain junction impedance comparable to the antenna resistance (100 Ω) while adjusting the capacitance. The response time would then be given by $RC = 10^{-12}$ A. (A in μm^2)

We have considered several FIR functional circuits; these have not yet been built. However, fabrication would require two successive photolithographically defined metalizations. The first capable of forming and supporting a stable barrier layer about 10 Å thick and the second of adhering to the substrate and making good contact to the barrier layer. One circuit usable as a parametric subharmonic generator might consist of a circle half made of each metal, overlapping at one intersection to form a small area MOM diode and at the other a large area ohmic contact. Inherent inductance and capacitance of this circuit and junction can make it resonant in the FIR. With appropriate input driving signal and bias leads and a realizable junction nonlinearity, a Q of 5 would be adequate to cause oscillation at half the signal frequency.

Some particularly interesting recent work has been with high speed deposited negative resistance junctions formed by evaporating a narrow lead stripe on tin with a thin surface oxidation. This junction is cooled to about 2°K where both metals are superconducting and irradiated with a focused argon laser beam; definite non-thermal response was observed. Responses of lead on aluminum junctions were observed, again at 2°K (aluminum above its superconducting transition). The response to X-band and 5145 Å argon laser radiation was very similar showing peaks in exactly

the same locations. The principal structural response occurs at dc bias voltage less than 20 mv and is due to the superconducting transition and photon scattering in the lead film.

A theoretical analysis[2] of the MOM antenna/diode as a detector of microwave and infrared radiation is being conducted and FIR experiments evaluated to examine the consistency of the theory. The antenna is coupled directly into the diode. An equivalent circuit is used to represent the system of the antenna and its coupling to the diode. A Stratton[3] tunneling model represents the nonlinear character of the junction. Detector performance is shown to obey experimentally verified laws and determine an optimum junction thickness and area for each frequency. It is shown that the detectivity at room temperature can be as high as 10^{10} watts^{-1} Hz$^{1/2}$ at frequencies of 10^{14} Hz in the infrared. Experimental results show that for small focusing angles, $\Theta_f = D/f$ (where f = 12.7 cm in this case), the efficiency η_0 is proportional to Θ_f^2 (see Fig. 1) consistent with the concept of effective aperture. The proportionality constant (at 337 μm wavelength) agrees within a factor of two with that expected from our theory; this discrepancy may be caused by uncertainty in the calorimetric laser power measurement. As the focusing angle is increased to the width of the major radiation lobe, the coupling efficiency saturates to about 3%, in agreement again with the theory. Different antenna lengths give proportionally different coupling efficiencies for small focusing angles and the same saturated value for larger angles.

To confirm that the FIR detection arises from the same mechanism as that for rf detection (i.e. rectification), we checked, using a balancing technique, that the same detected voltage comes from an rf signal as from a preadjusted ir signal, as the bias is increased up to about 100 mV.

This balancing technique has been applied to the study of the type of printed diodes integrated to an antenna described in Ref. 4. Preliminary

results show that some structures have coupling efficiencies as high as 2 or 3%, comparable to that of the mechanical point contact diode. This technique is applicable regardless of the nature of the rectification mechanism as long as it is the same at rf and ir frequencies. For example, we have also fabricated antenna structures where the detecting element is an evaporated micron-sized, thin-film wire without a junction. A weak bolometric response, with the same bias dependence, was observed at both frequencies and the best coupling efficiency was found to be around 1%.

We have studied the behavior of the point contact diode nonlinearities by observing the bias dependence of the rectified signal when a known amount of rf power is coupled to the diode. These results can be compared with the predications of the tunneling model. Values for the barrier parameters are found to be reasonable.

The diode's I-V characteristic up to third order can be expressed as:

$$I = \frac{1}{R} (V + mV^2 + nV^3)$$

Then the rectified voltage, V_r, when an rf voltage $V_D \cos\omega t$ is coupled to these diode nonlinearities is given by

$$V_r = (m + 3n\, V_b) \frac{V_D^2}{2}$$

The experimental dependence of V_r on V_b shown in Fig. 2, can be approximated by a straight line in the low bias region. We can then obtain for the 2 K-ohm diode, $m = .16\ V^{-1}$ and $n = 1.81\ V^{-2}$.

These values for m and n, which are independent of the contact area, are in general agreement with those obtained from the model assuming reasonable values for the barrier parameters. From the tunneling model, we can express the average potential, ϕ_0, and thickness of barrier, L, as:

$$\phi_o = \frac{1}{4\sqrt{6n}} \ln \frac{324\, R_D a}{4\sqrt{6n}}$$

$$L = \frac{4\sqrt{6n}\,\phi_o}{1.025}$$

By estimating the value of contact area as $a = .1\ \mu m^2$, we can then obtain $\phi_o = .65$ ev and $L = 10.3$ Å which are quite reasonable and change only logarithmically with the estimated area. Furthermore, the value of the asymmetry factor, α, according to the theory is given by

$$\alpha = m\sqrt{6/n}$$

which, in the case of Fig. 2 , is equal to 0.29 and does not depend on the estimated area.

As the resistance of the diode is lowered by adjusting the pressure of contact, the value for n decreases monotonically. For example; if $R_d' = 50$ ohms we get $n = 1.39$ so that $\phi_o = 0.43$ eV and $L = 7.3$ Å. At these low values of L and ϕ_o, the W.K.B. approximation used in calculating the tunneling probability begins to lose its applicability.

We have shown that in agreement with the theory, the zero bias responsivity, β_i (=m), remains nearly constant as the resistance is varied over two orders of magnitude. By studying the laser rectification as the resistance of the diode, R_D, "relaxes" continuously and slowly (presumably keepin the same asymmetry factor α) from 10 to few thousand ohms, we were able to fit the result to the expression:

$$V_r = V_o\left(\frac{R_D}{R_D + R_A}\right)^2$$

with two adjustable parameters, V_o and R_A (antenna resistance).

A 2 x 2 array of antenna/diodes has been fabricated for ultimate use as a real time holographic imaging array. This is now being evaluated as individual infrared rectifier/mixers. In operation, two infrared beams differing by a microwave frequency will irradiate the array. From the amplified difference frequency we can obtain relative phase information of the two signals. This provides the information required to define and construct a real time hologram.

(1) D. A. Jennings, F. R. Peterson, K. M. Evenson, Appl. Phys. Letts. 26, 510 (1975).

(2) To be published.

(3) R. Stratton, J. Phys. Chem. Solids 23, 1177 (1962).

(4) J. Small, G. M. Elchinger, A. Javan, A. Sanchez, F. J. Bachner, D. L. Smythe, Appl. Phys. Letts. 24, 275 (1974).

Figure 1. The antenna/ diode efficiency is plotted as a function of iris diameter, D. It should be noted that saturation at high values of D comes from a combination of approaching the beam diameter and exceeding the width of the first lobe. The proportionality constant, .0035, is within a factor of two of the theoretical value.

Figure 2. The experimental dependence of V_r on V_b is presented. Diode resistance was measured as 2 KΩ and values of $m = .16\ V^{-1}$ and $n = 1.81\ V^{-2}$ were calculated from this plot.

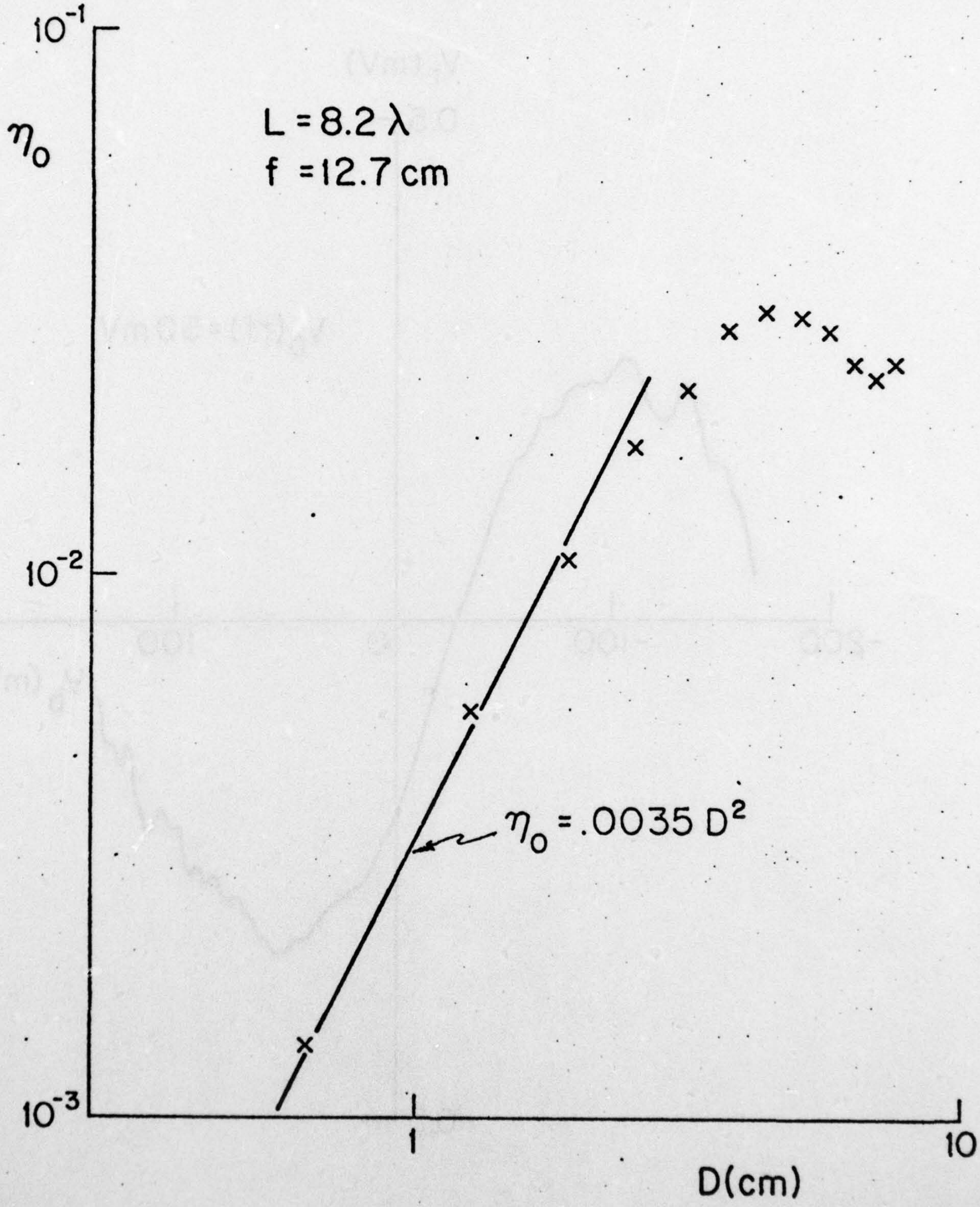

Fig 1

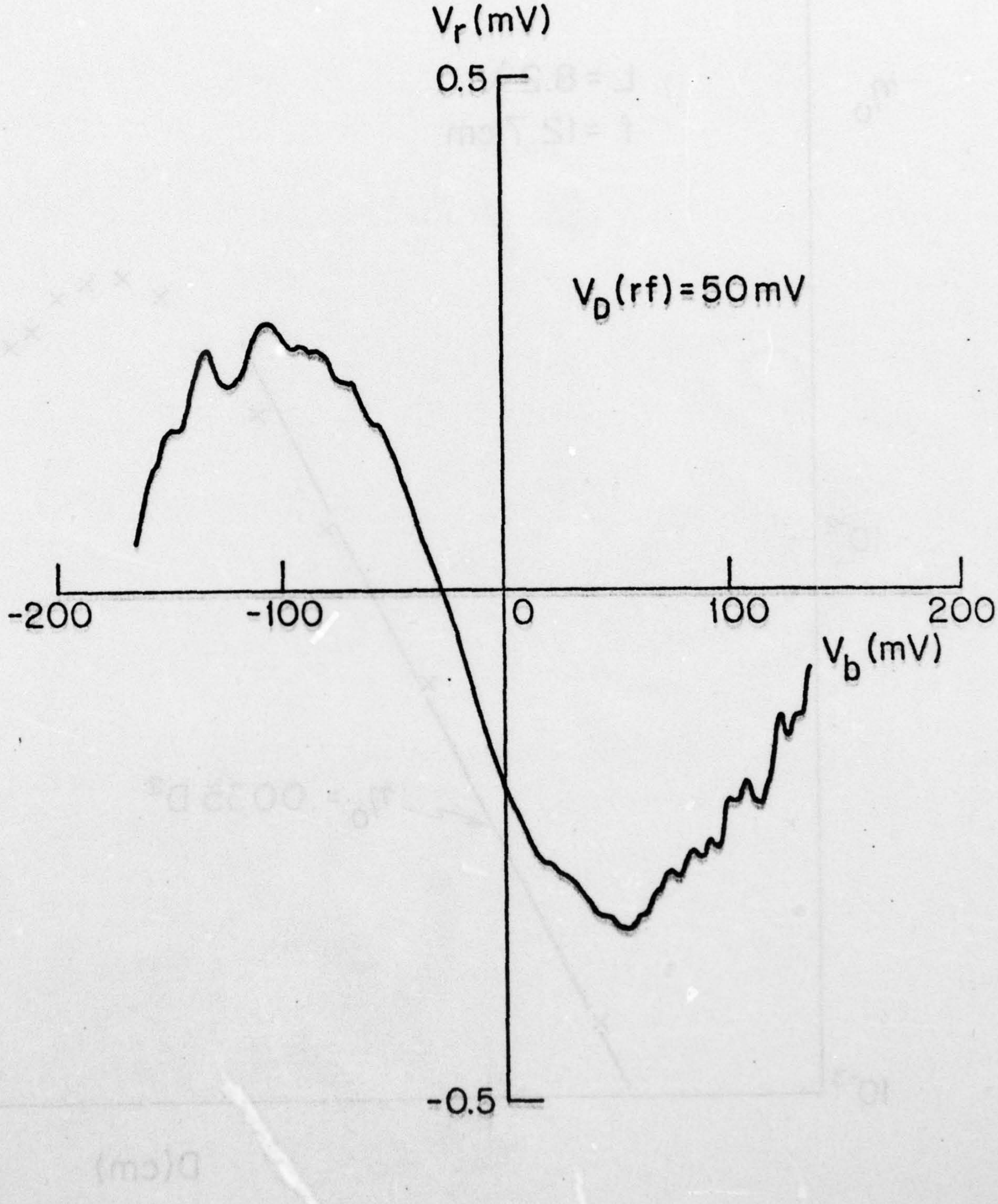

V_r (mV)
0.5
-0.5
$V_D(rf) = 50\,mV$
-200
-100
0
100
200
V_b (mV)